Physically Based Modeling of Delta Island Consumptive Use

A case study of Fabian Tract and Staten Island

By

Lucas Joseph Siegfried
B.S., Humboldt State University, 2008

THESIS

Submitted in partial satisfaction of the requirements for the degree of

Master of Science
in
Civil & Environmental Engineering
in the
Office of Graduate Studies
of the
University of California
Davis

Approved:

_____
Jay R. Lund, Chair

_____
William E. Fleenor

_____
Fabian A. Bombardelli

Committee in Charge
2012

Lucas Joseph Siegfried
December 2012
Civil & Environmental Engineering

Physically Based Modeling of Delta Island Consumptive Use
A case study of Fabian Tract and Staten Island

Abstract

Continuous water diversions, water operations, and land-use changes in the Delta have affected Delta water flows, quality, and suitability for native fish species. Knowledge and understanding of the flows in Delta rivers, channels, and streams is crucial to solve the Delta's many problems. In an on-going effort to better understand and manage the Delta, a collaborative, integrated approach was used to better predict internal Delta Island Consumptive Use of water (DICU) values and water quality variables on a higher resolution and base diversion and return locations on current high-resolution topography rather than past approximations. The Delta islands known as Fabian Tract and Staten Island were selected for this study based on available data and island accessibility. A combination of historical diversion and return location data, water rights claims, and LIDAR digital elevation model data were used to predict diversion and return locations on the islands. The accuracy of the predicted diversion and return locations was analyzed and improved through ground-truthing. To calculate water requirements and runoff returns from agricultural land-use, incorporating soil and land-use characteristics as well as weather data, the IWFM Demand Calculator (IDC) was selected. The choice was based on model capabilities, ease of use, applicability, and recommendations. As input to the IDC model, Fabian Tract and Staten Island were divided into grid cells forming subregions, representing fields, levees, ditches, and roads. The subregions were joined to form diversion and return watersheds representing the total area supplied by a given water source or the total drainage area for a given return. Diversion and return volumes were limited to physical abilities of the systems. Model results provide daily estimates of the volume of water diverted and returned from actual diversion and return locations, providing insights into daily agricultural diversion and return operations within the Delta that are missed in DICU models and supporting sustainable solutions for the problems of the Delta.

Acknowledgments

This report would not have been possible without support from the following people and agencies:

The State Water Resources Control Board

The Nature Conservancy

John Herrick, Esq., South Delta Water Agency, Stockton, CA.

Tariq N. Kadir, Senior Engineer, WR Chief, Integrated Hydrological Models Development Unit, Department of Water Resources Bay-Delta Office, Sacramento, CA.

Emin C. Dogrul, Water Resources Engineer, Hydrologic Models Development Unit, California Department of Water Resources Bay-Delta Office, Sacramento, CA.

Jay R. Lund, Director Center for Watershed Sciences, Ray B. Krone Professor of Environmental Engineering, Department of Civil & Environmental Engineering, University of California, Davis, Davis, CA.

William E. Fleenor, Professional Research Engineer, Department of Civil & Environmental Engineering, University of California, Davis, Davis, CA.

Fabian A. Bombardelli, Associate Professor, Department of Civil & Environmental Engineering , University of California, Davis, Davis, CA

Josue Medellin-Azuara, Assistant Project Scientist, Department of Civil & Environmental Engineering, University of California, Davis, Davis, CA.

Angeles Casas Planes, Center for Spatial Technologies and Remote Sensing, University of California, Davis, Davis, CA.

Table of Contents

Table of Figures

Table of Tables

1 Introduction

The Sacramento-San Joaquin Delta is upstream of the confluence of the Sacramento and San Joaquin Rivers in the Central Valley of California. Most water in California drains into the Sacramento-San Joaquin Delta or is diverted upstream of the Delta through a series of canals and aqueducts. These projects distribute the water to 25 million Californians for drinking, irrigation, and industry. In addition the Delta is home to over 500,000 people and over 750 species of flora and fauna (State of California 2007).

Prior to the influence of immigration, the Delta was a freshwater tidal marshland. The Delta was diked, drained, and dredged by European settlers between 1850 and 1920 for agriculture, navigation, and flood control. In the central and western Delta, the constructed levee and drainage systems consist primarily of peat soils (State of California 2007).

By the end of the 1930's, the channelization of the Delta had led to a group of about 57 land masses, 1,150 square-miles, of reclaimed land for agricultural use surrounded by water known as the Delta Islands (Thompson 1957; Whipple et al. 2012). Agricultural uses of the Delta Islands, starting in the 1850's, has resulted in their subsidence, with many central and western islands now 10 to 25 ft below sea level. The continuous subsidence in combination with sea level rise and imperfect levees continues to increase seepage rates into the islands from the surrounding channels and the likelihood of levee failures (Rojstaczer et al. 1991; Rojstaczer and Deverel 1993). In addition to the sea level rise and subsidence, continuous water diversions, water operations, and land-use changes upstream and within the Delta have impaired Delta water flows, quality, and suitability for many native fish species (Lund et al. 2007, 2010).

A thorough knowledge and understanding of flows in Delta channels and streams is crucial for solutions to Delta ecosystem problems (RMA 2005). It has long been recognized that in-Delta diversions and return flows have not been adequately estimated. These flows are currently aggregated at 142 locations in the Delta as monthly averages and are designated as Delta Island Consumptive Use (DICU). The 142 locations were chosen as a simple way to regionalize the Delta but currently are applied at up to 258 locations as internal boundary conditions in 1-, 2-, and 3- dimensional models applied to the Delta. The Delta Atlas identifies over 1800 diversion locations and references over 210 returns in the Delta, many of which are no longer serviceable due to age or location. Peak withdrawals are reported in the Delta Atlas as exceeding 4,000 cfs during summer irrigation periods, but DICU values are currently reported as not exceeding 2,100 cfs over a monthly average.

Recently, an improved integrated water flow model (IWFM) demand calculator (IDC) was released by the California Department of Water Resources (DWR 2011). IDC is a stand-alone model that computes root zone processes, deep percolation rates, and irrigation water requirements. Incorporating major agricultural and urban water demand parameters, including evapotranspiration (ET), IDC can solve the soil moisture

balance in the root zone, determine surface runoff resulting from precipitation and irrigation return flow, and compute agricultural and urban water demands. Through the use of IDC, the estimation of consumptive water demands in the Delta may be improved both spatially and temporally.

The work herein represents a proof-of-concept of an approach to produce more realistic DICU estimates and create a model that can easily be extended to other Delta islands. It incorporates improved consumptive use knowledge developed in IDC with drainage patterns extracted from recent LIDAR work on the islands, water quality data collected from the Municipal Water Quality Investigations (MWQI) program, and water quality data from the Moss Landing Marine Laboratory. The combination of annual cropping patterns and irrigation needs, coupled with the physical drainage characteristics, the agricultural water requirements developed in IDC, and the water quality data provides the first direct attempt to estimate the water quantity and quality effects of Delta return flows.

The objectives of this research are:

- To reduce the current uncertainty of DICU predictions spatially and temporally for modeling the Delta flows and quality.
- To implement a landscape scale, integrated approach to better predict DICU values and water quality variables by predicting both quantity and quality on a higher resolution time step than current monthly scales and basing both diversion and return locations on actual geography rather than simple geographical approximation.
- To produce a model that will accept better data to continue to improve DICU estimates without further fundamental model development.
- To discuss further data collection and model development to benefit water quality modeling predictions.

2 Background

The Sacramento-San Joaquin Delta is complex. To assist with understanding the complexities of the Delta, a background describing the location, subsidence, past DICU studies, and water quality concerns of the Delta is provided as well as a review of evapotranspiration and hydrological models.

2.1 Location

Formed by the confluence of the Sacramento and San Joaquin Rivers, the Sacramento-San Joaquin Delta is located along the western edge of the Central Valley in Northern California near where the rivers enter Suisan Bay (Figure 1). The Delta consists of numerous water ways creating an expansive inland river delta and estuary. Completely surrounded by the waterways are a group of land masses, known as the Delta Islands, that were developed from the peat and peaty alluvium soils deposited from the Sierra Nevada, Coast Ranges, and southern Cascade Range as well as accumulations of decaying marsh plants over several thousand years (State of California 2007).

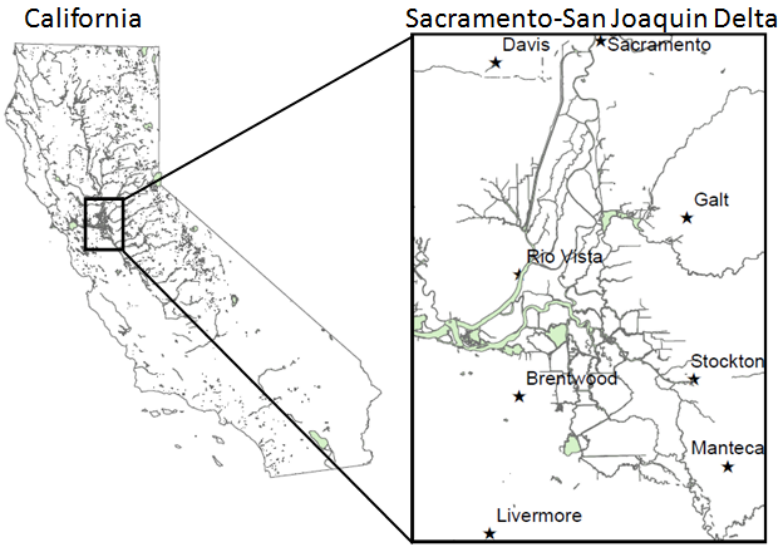

Figure 1. The Sacramento-San Joaquin Delta, depicting the channels and tracts which define the Delta as well as the Delta Islands.

2.2 Subsidence in the Delta

Originally freshwater tidal marsh, approximately 57 Delta islands or tracts are protected from water which surrounds them by more than 1,100 miles of levees (USGS 2000). Reclamation and agriculture on the developed islands in the central and western Delta have led to the subsidence of the land surface at long term average rates of 1-3 inches per year (Rojstaczer et al. 1991; Rojstaczer and Deverel 1993). As a result, many Delta Islands are 10 to 25 feet below sea level (Figure 2) (USGS 2000).

Figure 2. Subsidence on Staten Island, depicting a diversion siphon.

To prevent the islands from flooding internally and maintain adequate ground water levels for agriculture, an extensive network of drainage ditches and return pumps exist on these lands. Many Delta Island land elevations are below sea level and their neighboring channels so return pumps are often required to return accumulated water to the channels. Accumulated agricultural drainage is returned by pumping the water through or over the levees into the neighboring channels (Figure 3, USGS 2000). Additionally, due to the often higher neighboring channel elevations, much of the water consumed internally on the Delta Islands may be siphoned, opposed to pumped, onto the Delta Islands. The diverted water may then be run down-grade through a series of diversion ditches and piping for irrigation.

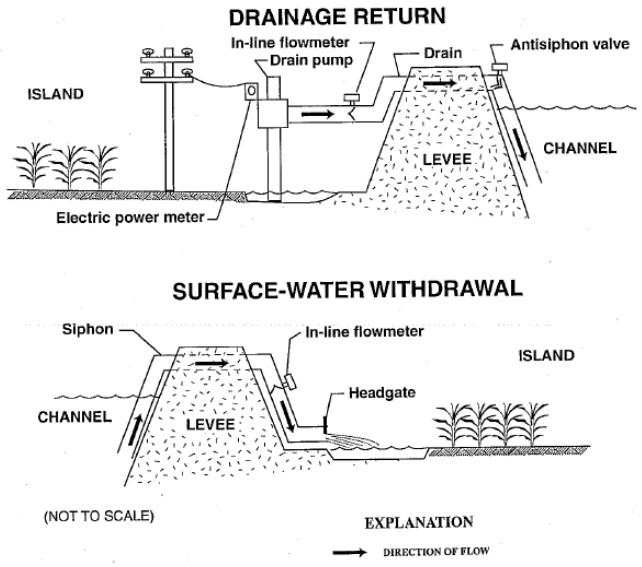

Figure 3. Diversion return pump and siphon schematic (Templin and Cherry 1997).

Prior to development, organic peat soils in the Delta were water logged and primarily under anaerobic conditions. As a result, organic carbon accumulation exceeded decomposition. Aerobic conditions, which favor rapid oxidation of the carbon in the peat soil, were introduced to the soil by the draining of the land for agriculture. Most islands were reclaimed early enough that the dense tule vegetation had to be burned off before tillage was possible. Early agricultural practices burned the stubble, and some of the peat soil, every 2-3 years to control crop disease (USGS 2000).

The continuous use of Delta Islands for agriculture has led to the decomposition of the organic peat soils, resulting in the release of carbon-dioxide gas to the atmosphere, island subsidence, and reductions in organic soil thickness (USGS 2000; Deverel and Rojstaczer 1996). Reductions in organic soil thicknesses are suspected of attributing increases in wet areas on Delta Islands from increased seepage under levees. The cumulative acreage of wet areas on Delta Islands was estimated to have increased linearly nearly 19-fold to 5,655 acres in 2011. Additionally, nearly 30,000 acres are projected to be vulnerable to reduced arability and increased wetness by 2050. Furthermore, regression analysis has suggested nearly 14,000 acres could become too wet to farm by 2050 (HydroFocus, Inc. 2012).

Loss of suitable agricultural land, decreased levee stability, and additional farming expenses from Delta Island subsidence, as well as the passage of California Assembly Bill 32 which created the potential to trade credits for carbon sequestered in wetlands on subsided delta islands, has led to interest to stop and reverse the effects of delta subsidence (Deverel 2012; HydroFocus, Inc. 2012). The use of managed impounded marshes can restore most of the central delta and a large portion of the western Delta to sea level within 50 to 250 years. Using managed impounded marshes, carbon sequestration rates would range from 12 to 15 tons carbon per hectare-year and levee stability would be increased (Deverel 2012).

2.3 DICU

To better understand and manage the Delta, DICU has been studied: Owen and Nance (1962) monitored surface inflow, drain discharge, precipitation, changes in soil moisture content, weather data, and cropping patterns and methods on Twitchell Island to add clarity to DICU water supply and utilization characteristics; the State of California Department of Water Resources Division of Planning (SDWR) (1995) developed a DICU model to estimate Delta agricultural diversion and return volumes on a spatial level and assign these volumes and predict water quality; and Templin and Cherry (1997) used electrical power-consumption records to estimate drainage return volumes and physically measured select surface-water withdrawals on Twitchell Island to develop a better understanding of DICU. This section examines these case studies.

2.3.1 Hydrology of the Sacramento-San Joaquin Delta

Between October 1959 and March 1961, a hydrologic investigation of Twitchell Island was done on DICU water supply and utilization characteristics, considering the relationship between consumptive use on the island and net depletion from the surrounding channels to be paramount (Owen and Nance 1962). To assess all water sources and types of water utilization, the following variables were monitored: surface inflow, drain discharge, precipitation, changes in soil moisture content, weather data, and cropping patterns and methods. Sources of water considered included siphon inflow, seepage, and precipitation. Types of water utilization considered included evaporation and transpiration (ET), and pump outflow (return flow). Changes in the soil moisture and ground water storage were also considered, forming the following hydrologic mass balance equation:

$$\text{Water Supply} = \text{Water Utilization}$$

$$\text{SI} + \text{S} + \text{P} = \text{CU} + \text{PO} + \Delta\text{SM}$$

where

SI = siphon inflow
S = seepage
P = precipitation
CU = consumptive use (ET loss)
ΔSM = change in soil moisture
PO = pumped outflow (return flow)

Various methods were used to monitor agricultural practices on Twitchell Island. Operation of siphons, varying in diameter from 6 to 14 inches, for surface irrigation water on Twitchell Island was found to be random. Thus to record siphon use, springs and bellows were utilized to actuate recording vacuum gages. Seepage rates were not directly measured, but ground water pressure field tests provided estimates of soil transmissibility. From these field tests, 90 percent of the water permeating into the island was determined travel horizontally through underlying sands and then vertically upward through an upper organic mantel 30 to 40 feet in depth. Combining the developed groundwater flow patterns with measurements of the surrounding channel mean surface water elevation and free groundwater elevations within the islands,

Darcy's Law was used to develop a distribution of monthly subsurface inflow during the study period. Precipitation was recorded through five rain gages. Total rainfall on the island was estimated using Thiessen Polygons. ET estimates were made by combining weather station observations with different estimation methods including the Blaney Criddle formula, pan evaporation correlation, precipitation-evaporation index, and the modification of previous estimates. Additionally, an attempt was made to estimate ET from ground cover but was not completed. Pump outflow was computed by using historical energy records combined with known pump efficiencies and pumping heads. From Delta soil studies, the soil moisture content was found to commonly range between 500 and 2,000 percent of dry weight, and significant soil moisture storage above the free groundwater was possible. Thus, aluminum tubes were driven seven feet into the ground at 60 different locations on the island and a neutron probe was used to make soil moisture readings whenever practical.

Three conclusions were drawn from this hydrological investigation of Twitchell Island (Appendix A): 1) the rate of consumptive use is not necessarily the same as the rate of channel depletion in the Delta; 2) changes in soil moisture need to be considered in computing net channel depletion; 3) and including soil moisture in computations is expected to increase the computed value of net channel depletion from the Delta during critical water supply months but decrease the computed value of net channel depletion in the non-critical months.

2.3.2 Estimation of Delta Island Diversions and Return Flows

A model to estimate Delta diversion and return volumes on a spatial level and assign these volumes and associated water quality concentrations to model nodes was developed by the DWR (1995). For the model, the Delta was subdivided into 142 regions or subareas. Consumptive use of water for each subarea was then calculated using monthly time steps accounting for precipitation, seepage, ET, irrigation, soil moisture storage, leach water, runoff, crop type, and acreage. Total consumptive use (TCU) satisfies a water budget accounting for DICU runoff, seepage, and applied water. Diversion and return flows for each subarea were calculated by an associated routine (NODCU) and then allocated to approximately 250 diversion and 200 drainage nodes. Results from the DICU model were then used as input into the DWR Delta Salinity model to perform historical simulations and planning studies.

Given ET, precipitation (CU_p), runoff (CU_R), seepage (CU_S), and change in the soil moisture content (ΔSM), the minimum irrigation (IR) was determined by combining the following equations:

$$\mathrm{TCU} = \mathrm{CU_P} + \mathrm{CU_S} + \mathrm{CU_{AW}} + \Delta\mathrm{SM} = \mathrm{ET} + \Delta\mathrm{SM}$$

$$\mathrm{I_R} = \mathrm{CU_{AW}} + \Delta\mathrm{SM}$$

Assuming a farm irrigation efficiency factor and using the calculated minimum irrigation requirement, the Delta Island diversions and drainages were then calculated using NODCU (Appendix B).

The study results indicated that a DICU model can estimate Delta hydrodynamic inputs as well as water quality and practical fate and transport on a detailed spatial level provided detailed land use, farming practices, and climatic data. The developed DICU model represents moisture changes reasonably well on Twitchell Island. However, the model tends to over predict water requirements in the early growing season and under predict water requirements in the late growing season; additionally, seepage and return volumes are consistently under predicted. The current model is sensitive to changes in evapotranspiration and irrigation efficiency during the growing season as well as leaching practices following the growing season; DICU estimates are sensitive to seepage; and, finally, irrigation demands met through seepage and diverted water must be disaggregated to accurately simulate the importance of agricultural diversions on practical fate and transport.

2.3.3 Drainage-Return, Surface-Water Withdrawal, and Land-Use Data for the Sacramento-San Joaquin Delta, with Emphasis on Twitchell Island, California

A study of the Delta water use employed electrical power-consumption data to estimate drainage returns physically; measured selected surface-water withdrawals; digitized historical land-use maps from 1968; and compared historical maps with existing digital land-use maps from 1991 (Templin and Cherry 1997). Based on existing data and accessibility, Twitchell Island was selected for the study. Between March 1994 and February 1996, measurements of monthly drainage returns and surface-water withdrawals were made. At drain sites, flow meters were used to measure flows discharged by the main pump and auxiliary pump at the drain site. Additional estimates of monthly returns throughout the Delta were calculated from electric power-consumption data with pump-efficiency test data.

For the 1995 calendar year, a total drainage return of approximately 11,200 acre-feet was measured for Twitchell Island. In comparison, a total drainage return of 10,600 acre-feet, approximately 5 percent less than that measured, was estimated from power-consumption data. Monthly surface-water withdrawals, measured from 12 of the 21 known siphons on Twitchell Island, totaled about 2,400 acre-feet for 1995. Comparing the historical land-use map of the Delta to the 1991 digitized map, native vegetation in the Delta decreased by 25% from 1968 to 1991, while grain and hay crops within the Delta increased by 340%. Specifically for Twitchell Island, field crop acreage increased by about 44 % contributing to a 77% decrease in native vegetation on Twitchell Island.

2.4 Delta Water Quality

Discharges of water and nutrients from agricultural activities can affect stream water quality, but the scale of these effects is challenging to predict (Owen and Nance 1962; Jordan et al. 1997). Agricultural water can be withdrawn from surface and subsurface

sources. Although surface water diversions for agricultural use are regulated to an extent, historically regulation of groundwater and surface diversions has been separate. Many surface water returns from agricultural runoff are unregulated. Although water is diverted for agricultural use, and some of that water returns with impaired water quality, this gap in the regulation of water diversions and returns has made predicting agricultural discharges of water and nutrients to streams difficult (Madani and Lund 2011; Marvin Jung and Associates 2000).

The Sacramento-San Joaquin Delta is dominated by agriculture at the heart of California's water conveyance system and is the subject of many studies (Owen and Nance 1962; Kadir 2006; Marvin Jung and Associates 2000; SDWR 1995; Templin and Cherry 1997). Owen and Nance (1962) found that 2.43 ft of water per acre was consumed by agriculture on Twitchell Island during 1960. In 1960, the Delta had roughly 738,000 acres of agricultural land and conveyed 12 million ac-ft of water, exports and outflow (Owen and Nance 1962). Assuming that the value of consumptive use from Owen and Nance is applicable to the entire Delta for 1960, 1,793,340 ac-ft of water was consumed by Delta agriculture during 1960, roughly 15 percent of water conveyed through the Delta.

Despite the uncertainty in nutrient loading from agriculture to streams, agricultural land-use has increased nutrient delivery and accelerated eutrophication. Greater amounts of nitrogen and other nutrients are found in watersheds with more agricultural land-use (Jordan et al. 1997). Agricultural land-use nutrient export coefficients have been developed. However, these coefficients may poorly predict fluvial nutrient loading because nutrient export rates can vary significantly (Beaulac and Reckhow 1982). In addition, agricultural runoff can contain toxic chemicals which affect fluvial systems in a poorly understood manner (Baker and Johnson 1983). Most chlorinated–hydrocarbon pesticides have been replaced by biodegradable compounds, such as organophosphates characterized as 'extremely noxious, but labile compounds' (Lenat and Crawford 1994). These compounds can affect fluvial ecosystems and have sublethal effects at low pesticide concentrations (Lenat and Crawford 1994).

Recognition of changing demands of agriculture has led to more sustainable practices and government incentives to farmers for "green practices." In the United States, from 1980 to 2001 nitrogen-fertilizer efficiency of maize has increased by 36% as a result of education and large investments in soil testing and fertilizer application. Technologies that maintain or increase crop yields, such as drip and pivot irrigation, which can improve water-use efficiency and decrease salinization, have come to use in industrialized nations on high-value horticultural crops. Developed countries, such as Australia, Canada, European Union countries, Japan, Norway, Switzerland, and the United States sometimes provide payments to farmers who adopt environmentally sustainable farming practices (Tilman et al. 2002).

Delta water quality has historically been of concern, and remains so. Numerous studies have examined agricultural runoff within the Delta and water quality impacts on crop

production. Two recent studies of agricultural runoff in the Delta include Trihalomethane Formation Potential in the Sacramento-San Joaquin Delta Mathematical Model Development (DWR 1991) and Revision of Representative Delta Island Return Flow Quality for DSM2 and DICU Model Runs (Marvin Jung and Associates, Inc. 2000). Two studies of the water quality effects on crop production include Salt Tolerance of Crops in the Southern Sacramento-San Joaquin Delta (Hoffman, 2010) and 8.1 Analysis of Crop Salt Tolerance Data (Van Genuchten and Hoffman, 1984). This section reviews these studies.

2.4.1 Trihalomethane Formation Potential in the Sacramento-San Joaquin Delta Mathematical Model Development

A drinking water standard of 0.1 milligrams per liter for Trihalomethanes (THM[s]) was established by the Environmental Protection Agency in 1979. Concerns of a more stringent revision to this standard and problems for Delta Water users to meet the new standard led to a study of THM precursors in Delta channels (DWR 1991). This study was to better understand THM interactions within the Delta.

A mathematical model simulated the fate and movement of THM precursors throughout the Sacramento-San Joaquin Delta and predicted THM formation potential (THMFP) at Delta locations. The goals of the model were to quantify THM precursor contributions from freshwater inflows, agricultural discharges, and tidal influences at select export locations; evaluate the benefits of source water management alternatives at export locations to control THM precursor concentrations; and provide a guide for determining spatial and temporal distribution data and setting data collection priorities.

To model THMFP, the total potential amounts of THMs that can be produced on a molar basis (precursor effects) were simulated. Precursor effects can be influenced by the organic content of source water. To model these effects, established THM formation potential test conditions and inorganic sources of chlorine demand were modeled through the use of a simulation parameter called the total formation potential carbon (TFPC). The influential effects of bromide on the formation of THM were also simulated. The potential influence of bromide on the formation of THM was modeled through the use of a surrogate simulation parameter, chloride, and calculated parameters known as the Bromine Incorporation Factor and Bromine Distribution Factors. Using a data base of more than 200 observations in the Delta from 1983 to 1990, the Bromine Incorporation Factor was estimated to be a nonlinear function of the ratio between chloride and TFPC molar concentrations whereas the Bromine Distribution Factors were found to be functions of the Bromine Incorporation Factor. The fate and movement of precursor effects and influential effects of bromide from the upstream model boundaries to downstream export locations were modeled using a numerical model developed by DWR to simulate hydrodynamics and water quality within the Sacrament-San Joaquin Delta, known as DWR Delta Simulation Model (DWRDSM).

The model provided insight into precursor concentrations, bromide concentrations, and resulting THMFP distributions at different stations. Simulations performed to illustrate

the potential model utility showed that agricultural drainage was influential at locations where model deviation was greatest. These observations highlighted the need for more accurate agricultural drainage quality and quantity data in the Delta and suggested that modifications to the current Delta water system may be required for Delta Water users to be able to meet the new THM standard.

2.4.2 Revision of Representative Delta Island Return Flow Quality for DSM2 and DICU Model Runs

In 2000, monthly representative drain water quality values in the Delta were developed for computer models by tabulating existing Delta drain water quality; determining correlations between drain water quality parameters; tabulating historical EC data for Delta agricultural drain water for each municipal water quality investigation (MWQI); and using Delta Island monthly average drain water quality values to compute monthly average values for other mineral constituents in drain water (Marvin Jung and Associates Inc. 2000).

From this analysis, dissolved organic carbon (DOC) concentrations in the Delta agricultural drainages appeared to be related to location, season, soil type, and land surface elevations. Higher DOC concentrations were found in drain water during the winter whereas lower observed DOC concentrations were found during the summer, attributed to the pumping off of drain water. Additionally, higher DO concentrations were found on lower elevation islands and tracts, with surface elevations below mean sea level.

Data collected by the MWQI from 1991 to 1997, including 953 samples, were used in a regression analysis of DOC, trihalomethane formation potential carbon (TFPC), and ultraviolet absorbance at 254nm (UVA-254nm) to determine if there was a relationship between each set of variables. The regression analysis produced good correlation between these variables (Appendix C).

To assess correlations among drain water mineral constituents, the MWQI collected EC, TDS, Br, Ca, Mg, Na, and SO4 measurements for islands and tracts in the northern, western, and southeastern Delta. In the Western Delta's drainage, EC, TDS, Br, Cl, and Na, correlated well with all constituents with the exception of Ca; Ca correlated well with Mg and SO4; Mg and SO4 correlated well with all constituents. In Northern Delta drainage, EC and TDS correlated well with all constituents with the exception of Br; Br correlated well with Cl and Na; Ca correlated well with all constituents with the exceptions of Br, Cl, and Na; Cl correlated well with EC, TDS, Br, and Na; Mg correlated well with all constituents except for Br, Cl, and Na; Na, correlated well with all constituents except for Ca, Mg, and SO4; and SO4 correlated well with all constituents except for Br, Cl, and Na. In Southeastern Delta Drainage, EC and TDS correlated well with all constituents; in addition to EC and TDS, Br correlated well with Cl and Na; with the exceptions of Br, CA and Mg correlated well with all constituents; Cl and Na correlated well with all constituents except for SO4; SO4 correlated well with EC, TDS, CA, and Mg (Appendix B).

2.4.3 Salt Tolerance of Crops in the Southern Sacramento-San Joaquin Delta

Scientific research was reviewed and analyzed to examine crop productivity with more saline irrigation water, particularly for the South Delta. Hoffman (2010) reviewed literature on the effect of salinity on irrigated crops under South Delta conditions; reviewed strengths and limitations of steady-state and transient models of the suitability of saline water for crop production; used soil information to estimate and describe the approximate area and behavior of saline and drainage-impaired soils; and, provided conclusions and recommendations to the State Water Resources Control Board.

Two important considerations were used to evaluate water quality for irrigation: salinity and sodicity. Salinity is the salt content of a fluid and reported as electrical conductivity in units of microSiemens per centimeter (μS/cm). Sodocity is the potential for an excess concentration of sodium to occur in soil leading to deterioration of soil structure and reduced permeability. Excess sodium can reduce infiltration rates such that crops cannot be adequately supplied with water or be drained. Additionally, solutes such as boron, sodium, and chloride have potentially toxic effects on plants through uptake from crop roots and accumulation in leaves.

Salinity, or salt stress, can damage crops in three ways: season-long crop response, varying seasonal crop response, and foliar damage. Season-long response described a constant agricultural response to salinity throughout the agricultural season whereas varying seasonal crop response described the variation of crop response to salinity which may vary throughout the growing and harvests seasons. Both season-long and seasonal crop response involve stunting of growth. Foliar damage occurs from plant wetting with saline water, often from sprinkler irrigation under hot, dry, and windy weather conditions. In this case, the relative crop yield, Y_r, when salinities exceed a given crops salinity threshold, was estimated as follows:

$$Y_r = 100 - b(EC_e - a)$$

where,

a = the salinity threshold expressed in deciSiemens per meter
b= the slope expressed in percentage per deciSiemens per meter
EC_e= the mean electrical conductivity of a saturated-soil extract taken from the root zone

2.4.4 Analysis of Crop Salt Tolerance Data

Concern for reductions in crop productivity from excess soil salinity led to a study coupling salt tolerance data with a salt tolerance model using a least-squares fitting method (Van Genuchten and Hoffman, 1984). To provide an efficient and accurate tool for quantifying unknown parameters that appear in different crop response functions and analyzing crop responses to salinity, a computer program was developed. A piece-wise linear response model was developed to incorporate salt tolerance and management strategy data collected over several years. The piece-wise linear response model was defined as follows:

$$Y_r = \begin{cases} 1 & 0 \le c \le c_t \\ 1 - s(c - c_1) & c_t \le c \le c_0 \\ 0 & c > c_0 \end{cases}$$

and

$$Y = \begin{cases} Y_m & 0 \le c \le c_t \\ Y_m - Y_m(c - c_t) & c_t \le c \le c_0 \\ 0 & c > c_0 \end{cases}$$

where

$Y = Y_r Y_m$ = Crop Yield
Y_r = Relative crop yield
Y_m = Yield under non-saline conditions
s = Absolute value of slope response function between c_1 and c_2
c =Average rootzone salinity
c_0 = Rootzone salinity at point crop yield is 0
c_t = Salinity threshold

In addition to the linear piece-wise model, for cases when more information is known and non-linear equations may be used, two non-linear but more accurate alternative models were developed which fit time-independent c_t and s directly to all data while still permitting Ym to vary from year to year. The first alternative model is

$$Y = \frac{Y_m}{1 + (c/c_{50})^{\rho}} \rightarrow Y_r = \frac{1}{1 + (c/c_{50})^{\rho}}$$

where

c_{50} = the salinity at which the crop yield is reduced by 50%
ρ = a crop dependent empirical constant

The second alternative model assumes an exponential relation between the yield and average rootzone salinity:

$$Y = Y_m e^{(\alpha c - \beta c^2)} \rightarrow Y_r = e^{(\alpha c - \beta c^2)}$$

where

α = crop specific empirical constant
β = crop specific empirical constant

2.5 Evapotranspiration

ET is the combined processes of liquid water changing phase to water vapor from free-water surfaces, evaporation, and the conversion of liquid water to water vapor through plant tissue, transpiration. ET is often one of the largest sources of water loss from soil. ET rates vary with vegetation and soil type(s) as well as the current meteorology and season, making ET difficult to estimate (Bedient et al. 2008).

The maximum water losses from ET occur when the water supply to plants and soil surface is unlimited. In such a case, the maximum possible water loss limited by meteorological conditions is referred to as potential ET (Thornthwaite 1984). Potential

ET can be estimated as the evaporation from a large, free-water surface such as a lake (Bedient et al. 2008). However, actual transpiration, which affects actual ET, is limited by the moisture supply available to plants which depends on plant characteristics, such as root depth, and the ability of the soil to transport water to the roots. Leaves of large surface areas under high temperature conditions can create transpiration rates that equal potential ET.

For most plants, transpiration occurs only during daylight, while photosynthesis is occurring, which can cause diurnal variations in groundwater levels in heavily vegetated areas. As soil moisture content falls below field capacity (moisture content above which water is drained by gravity), less water becomes available to plants which reduces transpiration by plants and reduces actual ET. If the soil moisture content becomes less than the wilting point (point at which the soil moisture content becomes too low for plants to extract further water) the plant will become starved for water and may die (Bedient et al. 2008).

In a natural system, the soil moisture content often changes with the seasons (Figure 4). When precipitation exceeds the rate of potential ET, precipitation recharges the soil moisture content until either the rainfall stops or the soil reaches field capacity, at which time all excess water turns to runoff. Water moves through soil relatively slowly leading to the upper soil layers recharging to field capacity prior to the lower soil layers. However, water from upper layers will continue to recharge the lower soil layers until the upper soil layer reaches a moisture deficit. When the rainfall rate is less than the rate of potential ET, the soil moisture content will reduce which can lead to a soil moisture deficit. Additionally, the ratio of roots to soil generally reduces with depth leading to slower reductions of the soil moisture content at deeper depths than at shallower depths. As a result, a soil moisture deficit typically occurs in the upper soil layers first (Bedient et al. 2008).

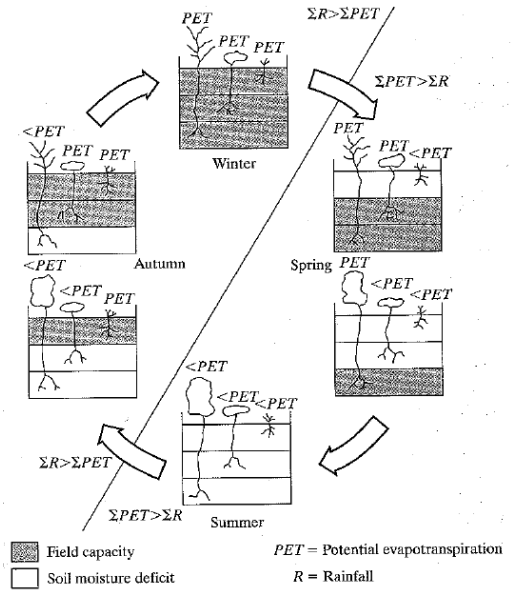

Figure 4. Example soil moisture cycle for three vegetation types (Bedient et al., 2008)

Techniques to estimate ET include an energy balance, a simplified method, meteorological data, eddy correlations, and soil water balance. This section examines each of these ET estimation methods.

2.5.1 Energy Balance

For seasonal, monthly, and daily estimations of ground-based ET, meteorological data can be used to make temporal interpolations. The ratio of latent heat flux to available energy for convective fluxes, known as the evaporative fraction, EF, is nearly constant during the daytime, allowing estimations of average daytime evaporation from one or two estimates of EF at midday (Crago 2000):

$$\mathrm{EF} = \frac{\mathrm{LE}}{\mathrm{Rn} - \mathrm{G}}$$

Using the evaporative fraction, ET is can be determined as (Courault et al. 2005)

$$\mathrm{ET} = \mathrm{EF} * \mathrm{Rn}$$

where

$$\mathrm{Rn} = \mathrm{LE} + \mathrm{H} + \mathrm{G}$$

and

Rn = available net radiant energy
G = soil heat flux
LE = latent energy exchanges
H = sensible heat flux.

Characterizing the energy balance equation in terms of the incident solar radiation, R_g; incident atmospheric radiation over the thermal spectral domain, R_a; surface albedo, α_s; surface emissivity, ε_s; and surface temperature, T_s, the energy balance equation is as follows (Courault et al. 2005):

$$\mathrm{Rn} = (1 - \alpha_s)\mathrm{Rg} + \varepsilon_s \mathrm{Ra} - \varepsilon_s \sigma \mathrm{T}_s^4$$

A multilayer approach, discriminating between soil and vegetation, or a single layer approach considering the soil and vegetation as a single component, can characterize the sensible heat flux and determine the available net radiant energy. For multilayer approaches, models have been developed to integrate the difference between the soil and canopy aerodynamic resistances with their corresponding temperatures (Courault et al. 2005). For single layer approaches, aerodynamic resistance, r_a, between the surface and a reference height in the lower atmosphere above the observed surface is considered as a single component to estimate the sensible heat flux where (Norman and Becker 1995):

$$\mathrm{H} = \rho c_p \mathrm{p}\,(\mathrm{T}_s - \mathrm{T}_a)/\mathrm{r}_a$$

where

ρ = air density
c_p = specific heat of the air

p=pressure at the surface
T = aerodynamic surface temperature and atmospheric temperature

Ignoring the second order dependence of aerodynamic resistance, an estimation of instantaneous latent energy exchanges can be made where (Courault et al. 2005)

$$LE = Rn - G - \rho cp(T_s - T_a)/r_a$$

Alternatively, the air vapor pressure, e_a, and a water vapor pressure exchange coefficient, h_s, can be used to estimate the instantaneous latent energy exchanges such that (Courault et al. 2005):

$$LE = \rho c_p h_s(e_s * T_s - e_a)$$

where

e_s*T_s= saturated vapor pressure at the surface temperature T_s

2.5.2 Simplified Method

A simplified method was derived to map daily ET over large areas from surface temperature data assuming that daily ET can be directly related to the instantaneous difference between the surface and atmosphere temperatures, the ratio of H to R_n is constant over the course of a day, and daily values of heat flux are negligible (Jackson et al. 1977):

$$ET_d = Rn + A - B(T_s - T_a)_i$$

where

A and B = Local calibration constants.

The calibration constants, which vary significantly based on location and climatic conditions, have been estimated under many different conditions (Courault *et al*. 2005).

2.5.3 Meteorological Approach

ET can be estimated from a reference ET value, ET_0, and a crop specific coefficient, K_c (Allen et al. 1998):

$$ET = K_c ET_0$$

The crop specific coefficient is determined from correlating measured ET values from a crop of interest to ET_0 values measured from a reference crop during the same time period. Taking into account factors such as soil moisture, crop maturity, wind, and relative humidity, the crop specific coefficient can be defined as follows (Allen et al. 1998):

$$K_c = K_{cb}K_s + K_w$$

where

K_{cb}= basal crop coefficient for crop c

K_s= water stress factor
K_w= soil water content factor

ET_0 is a representation of the evaporative power of the atmosphere for given climatic conditions and can be estimated by using the Penman-Monteith equation and measured meteorological climatic parameters (Allen et al. 1998):

$$ET_0 = \frac{1}{\lambda}\frac{\Delta(Rn - G) + \rho_a c_p \frac{e_s - e_a}{r_a}}{\Delta + \gamma\left(1 + \frac{r_s}{r_a}\right)}$$

where

λ = latent heat of vaporization
Δ = slope of saturation vapor pressure temperature
γ = psychometric constant
(e_s-e_a) = vapor pressure deficit of the air.

Incorporating equations for aerodynamic and surface resistance, the Penman-Monteith equation can be modified where (Sclanlon et al. 2005)

$$ET_0 = \frac{0.408\Delta(Rn - G) + \gamma\frac{900}{T + 273}u_2(e_s - e_a)}{\Delta + \gamma(1 + 0.34u_2)}$$

2.5.4 Eddy Correlation Method

ET can be estimated by averaging the movement of humidity from eddies and determining the net flux of water vapor upward using the Eddy Covariance Method or Eddy Correlation Method (Evett 2000):

$$ET = \left(\frac{M_w}{M_a p}\right)\rho_a\overline{w'e_a'}$$

where

$\overline{w'}$= average vertical wind speed
$\overline{e_a'}$= average water vapor pressure
M = molecular weights of water and air respectively.

2.5.5 SEBAL

Spectral radiances recorded by satellite-based sensor and meteorological data can be used to solve the Surface Energy Balance Algorithm for Land (SEBAL), determining water consumption or actual evapotranspiration as well as biomass production of agricultural crops and native vegetation at a given resolution. In some cases, yield can also be determined from biomass production. Here ET is determined as a residual of the surface energy balance, accounting for radiative, aerodynamic, and energy balance physics. All input parameters, with the exception of ground-based weather data, are acquired by satellite, thus knowledge of land use and crop types is not required to determine ET (SEBAL North America 2012).

2.5.6 Soil Water Balance

By conservation of mass, ET can be estimated as follows:

$$ET = P - R_0 - D - \Delta S$$

where

P = precipitation
R_0= runoff
D = drainage below the root zone
ΔS = change in soil water storage

During dry periods, runoff and precipitation are zero; therefore ET can be estimated as the change in water storage minus the drainage from the soil water storage. Assuming that the drainage is zero, ET can be estimated as the change in water storage during dry periods (Sclanlon et al. 2005).

2.5.7 Comparison of Methods

A summary of the ET estimation methods, including respective a brief description of the methods approach and requirements, is presented herein (Table 1). Each method uses a different approach, requiring different information to determine ET.

Table 1. Summary of ET estimation methods.

Method	Approach	Requirements
Energy Balance (Section 2.5.1)	Temporal interpolation from energy balance equations	Evaporative Fraction, available net radiant energy
Simplified Method (Section 2.5.2)	Temporal estimation from local calibration constants	Available net radiant energy, aerodynamic surface temperature and atmospheric temperature, local calibration constants
Meteorological Approach (Section 2.5.3)	Estimation from reference ET and a crop specific coefficient	Reference ET, crop specific coefficient
Eddy Correlation Method (Section 2.5.4)	Estimation from averaging the net flux of water vapor upward through eddies	Molecular weights of water and air, air pressure at the surface, density of air, average vertical wind speed, average water vapor pressure
SEBAL (Section 2.5.5)	Estimation from the Surface Energy Balance Algorithm for Land using spectral radiances and meteorological data	Spectral radiances recorded by satellite-based sensor and meteorological data, excluding ground-based weather data and land use data
Soil Water Balance (Section 2.5.6)	Estimation from conservation of mass	Precipitation, runoff, drainage below the root zone, and change in soil water storage

2.6 Flow and Water Quality Models

Models have been developed to simulate agricultural water demands using soil water budgets. Three such models are examined herein: Delta Evapotranspiration of Applied Water model (DETAW), IWFM, and MODFLOW.

2.6.1 DETAW

DETAW was recently released by DWR and UC Davis to enable consistency between the Department of Water Resources models CalSim-II and DSM2 as well as to improve the estimation of consumptive water demands in the Delta for the two models spatially and temporally (IHMD 2011). DETAW uses a graphical user interface (GUI) written in C++ to allow for input data modifications and graphical viewing of a wide array of computed results (Kadir 2006).

Daily soil water balances for 168 subareas within the Sacramento-San Joaquin River Delta region are calculated through the simulation of ET of Applied Water (SIMETAW) model with modifications to estimates accounting for ET losses and water contributions from rainfall, seepage, and irrigation. Daily ETAW for historical (time varying) and projected (fixed) land-use development levels may be calculated by DETAW using land and water use categories including eleven crop categories, urban land-use, riparian areas, and open water surfaces. Input parameters, such as precipitation and land-use, may be modified in DETAW to model alternative scenarios including climate change studies. Two Delta crop pattern extremes are considered by DETAW: critically-dry or wet years. For either case, estimation at the Delta Uplands and Delta Lowlands aggregate level is made to determine the total crop acreages by category (Kadir 2006).

2.6.2 IWFM

IWFM was developed and maintained by DWR. Originally known as the Integrated Groundwater-Surface water Model version 2 (IGSM2), IWFM was released to the public in 2002 by DWR as a FORTRAN-based mathematical surface-subsurface hydrologic model using an irrigation-scheduling-type approach to simulate ground water interactions including groundwater flow, stream flow, and surface flow. IWFM is a GNU licensed software, thus all of the source codes, executables, documentation, and training material are freely available to the public on the DWR's website (Dogrul et al. 2011; IHMD 2011).

IWFM can simulate groundwater elevation in a multi-layer aquifer system and the flows among the aquifer layers and can model stream flows and lake storages, incorporating their interactions with the aquifer systems by solving conservation equations for groundwater, streams and lakes simultaneously. Additionally, IWFM can simulate the water demand as a function of different land-use and crop types, comparing values to the historical or projected amount of water supply. This ability distinguishes IWFM from other ground water models by allowing users to specify stream diversion and pumping locations for the source of water supply, as well as the rate or quantity of water used at each location, over the modeled area. The quantity of infiltration, ET, and surface water runoff may then be computed based on the user specified precipitation and irrigation

rates as well as the distribution of land-use and crop types over the model domain. Furthermore, the recharge rates of water to groundwater may be computed by simulating the vertical movement of the soil moisture through the root zone and the unsaturated and saturated ground water system (Dogrul et al. 2011; IHMD 2011).

2.6.3 IDC

Recently IDC was released as a stand-alone root zone modeling tool by DWR to estimate irrigation water requirements and route the soil moisture through root zone in the context of integrated hydrologic modeling. Written in FORTRAN 2003, IDC uses an object-oriented programming approach that consists of input data files, output data files, a numerical engine to read data from input files, compute applied water demands, route water through the root zone, and print results to output files, and a user interface (IHMD 2011a).

IDC assumes that computed irrigation water requirements equal applied water. The underlying root zone simulation engine of IDC can be linked to an integrated hydrologic model, such as IWFM, to define the amount of applied water as the sum of simulated diversions computed by the integrated hydrological model. Based on the state of the aquifer and the stream flows, the amount of applied water can be less than or equal to the water demand computed by the root zone simulation engine. When using IDC to compute irrigation water requirements and route moisture through the root zone, either a regular or irregular computational grid is required. The grid cells created in IDC are grouped into user defined subregions that may represent different types of boundaries and scales such as delta islands, water districts, or counties. IDC allows for user defined time series land-use areas to be assigned to each grid cell, permitting time varying land-use conditions during a simulation period. Precipitation and applied water for all land-use types are routed through the root zone. Based on user input, surface runoff resulting from precipitation or irrigation at each cell may be routed to a subregion, another grid cell, or outside of the model area (IHMD 2011a).

2.6.4 MODFLOW

Published in 1984 by the U.S. Geological Survey (USGS), MODFLOW is a three-dimensional finite-difference ground-water model which uses a modular structure permitting modifications to adapt the code for particular applications. Since 1984, many modifications have been made to MODFLOW, increasing the program's capabilities (USGS 2011).

Updated in 2005, the current version of MODFLOW simulates steady and non-steady state flow conditions in an irregular shaped flow system in which aquifer layers can be unconfined, confined, or a combination of both. Flows from external sources, such as precipitation, ET, flow to drains, and flow through river beds, can also be simulated by MODFLOW. Spatial variability of hydraulic conductivities or transmissivities for any layer may be simulated with spatial variability. Additionally, hydraulic conductivities or tranmissivities can be modeled as isotropic and the storage coefficient can be defined as heterogeneous. To allow water to be supplied to a boundary block in the modeled area

at a proportional rate to the current head difference between the internal and external water levels, head and flux boundaries can be specified along with head dependent flux across the model's outer boundary (USGS 2011).

The ground-water flow equation is solved by MODFLOW by using finite-difference approximation. This approach divides the flow region into blocks in which the medium properties are assumed to be uniform throughout. Each block is defined by a grid of mutually perpendicular lines which may be variably spaced. Additionally, the model layers made up of blocks can be of variable thickness. For each block a separate flow equation is written and several solvers are provided for solving the resulting matrix problem. The solver for each particular problem is user specified and the flow-rate and cumulative-volume balances from each type of inflow and outflow are computed for each time step (USGS 2011).

2.6.5 MODFLOW with Farm Processes

Recently, MODFLOW was modified by the US Geological Survey to incorporate farm processes and effectively model the conjunctive use of surface and subsurface water resource requirements through the simulation of land-use-based root zone and surface flow processes as well as groundwater flows, stream flows, and their interactions (USGS 2011).

MODFLOW with Farm Process (MF-FMP) considers two types of water budgeting for control volumes horizontally delineated, irrigated and non-irrigated. MF-FMP does not include changes in soil-water storage and therefore only uses the land surface as a control interface. The water-accounting units are budgeted through the use of two approaches: mass balance and economic balance. The mass balance approach balances all physical inflow and outflow components to and from the control volume to meet budget constraints. The economic balance approach uses the irrigation water demand and the water supply from different surface or groundwater components to meet the budget constraints. MF-FMP simulates the land surface and vadose zone flow processes as well as water demands through a land-use based approach. Finite difference cells in MF-FMP are grouped into subregions referred to as "farms" distinguish the budget units for all physical flows into and out of a subregion, including natural and irrigation-induced delivery and return flows. Farms are used by MF-FMP to simulate the land surface and vadose zone flow processes as well as water demands through a land-use based approach (USGS 2011).

3 Methods and Procedures

The following major tasks were implemented to meet the objectives of this project:

1. Coordinate with the Water Board to select the best south Delta DICU graphical regions to be examined for this proof-of-concept effort.

2. Develop from existing GIS data and LIDAR the required topography to determine diversion drainage patterns. Confirm, as possible, drainage predictions with agricultural managers.
3. Select a model to incorporate the latest GIS along with cropping and irrigation schemes to predict return flows.
4. Use existing water quality data from MWQI and others to predict water quality of the return flows.

Each of these tasks is discussed in detail below.

3.1 Task 1: Selection of Study Location

Coordinating with The Water Board and The Nature Conservancy as well as considering data availability and island accessibility, Fabian Tract and Staten Island were selected for this proof of concept effort (Figure 5). Fabian Tract is located in the southern Delta between Brentwood, Manteca, and Livermore and has a total area of about 6580 acres, primarily used for agricultural purposes and suffering from subsidence with field elevations of about -9 to 3 feet and maximum levee elevations of about 33 feet. Staten Island is located in the central-east Delta and consists of about 9222 acres. Similar to Fabian Tract, the Staten Island primarily is used for agricultural purposes and is suffering from subsidence with field elevations of about -18 to 2 feet and maximum levee elevations of about 24 feet.

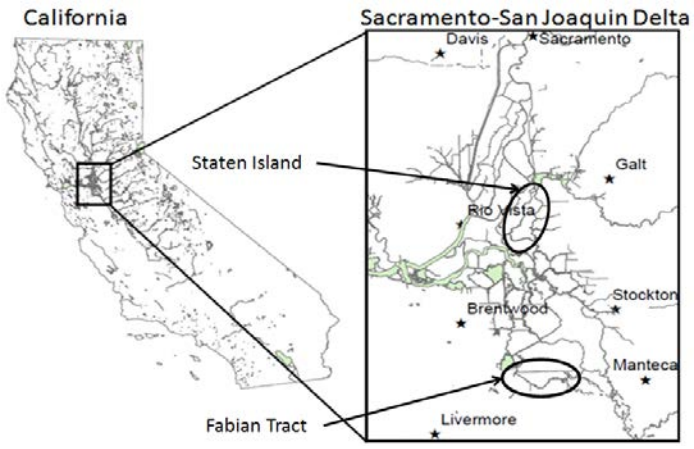

Figure 5. Staten Island and Fabian Tract, within the Sacramento-San Joaquin Delta were selected for this study.

3.2 Task 2: Development of Delta Island Topography

LIDAR digital elevation model (DEM) data and existing diversion and return data were collected and analyzed to identify likely diversion and return locations as well as field drainage patterns in a non-invasive manner. The validity of these predictions was then analyzed by ground-truthing.

3.2.1 Analysis of Existing Data

Diversion and return data were collected from the California Department of Fish and Game (DFG) and DWR. DFG place of use (POU) data, collected from 1993 to 2005, consisted of 5461 locations with a description of the location, owner, type of diversion or return, and use at each location. Water rights claims for 2011 were collected from the California Division of Water Rights and consisted of a description of location, right type, owner, activity, and use at each claim location. Comparing the DFG and DWR datasets through GIS analysis, deviations between the datasets are observed (Figure 6). Additionally, most locations provided by the DFG and DWR data are classified as diversions.

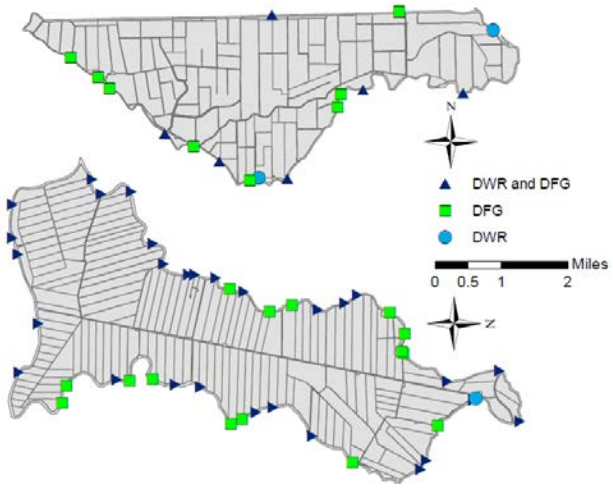

Figure 6. DFG and DWR published locations on Fabian Tract (above) and Staten Island (below).

3.2.2 ArcGIS Analysis

To determine agricultural return locations on Fabian Tract, an attempt was made to analyze DEM LIDAR data using hydrological analysis tools in ArcGIS, including the hill slope model, basin analysis, and sink analysis. However, the built-in ArcGIS hydrological tools failed to produce valid drainage results where hill slopes are very mild (slope<<1%), including Fabian Tract and Staten Island. These tools use DEM data to determine hill slopes and then compute drainage patterns across the terrain of interest based on the determined hill slopes, producing valid results in regions of significant hill slope but failing to produce valid results in regions of mild slope. To overcome the limits of the ArcGIS built-in hydrological tools, visual observation of island drainage patterns were made in ArcGIS and suspected return locations were examined with Google Earth (Figures 7, 8, 9, and 10).

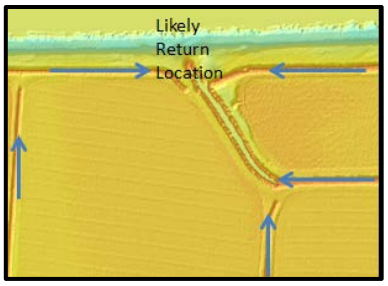

Figure 7. Observed drainage pattern on Staten Island.

Figure 8. Located return in Google Earth.

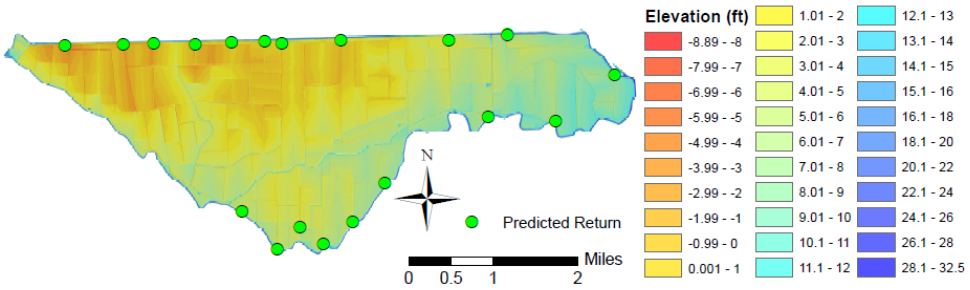

Figure 9. Predicted agricultural return locations from LIDAR on Fabian Tract.

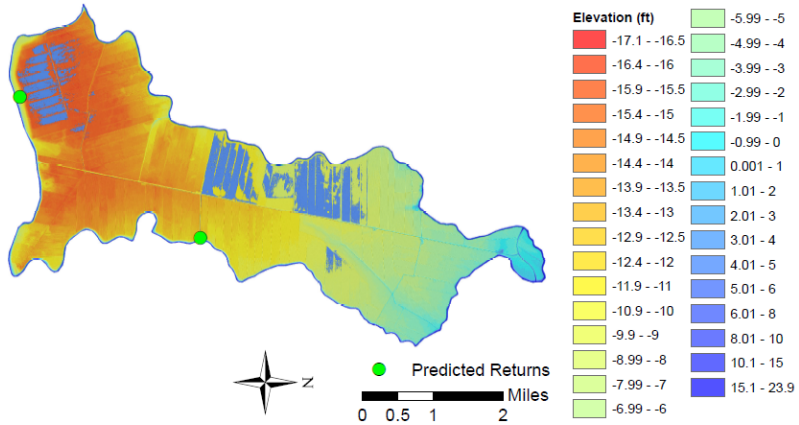

Figure 10. Predicted agricultural return locations from LIDAR on Staten Island.

3.2.3 Ground-Truthing

Ground-truthing was used to verify collected data and validate predicted return locations. To ground-truth Fabian Tract and Staten Island, permission to enter and examine the premises was first attained from the private land owners on the islands. Once permission to access the islands was granted, the each island was surveyed for existing diversion and return locations. Surveying included 1) validating or discrediting diversion and return locations; 2) visually examining the island for unmarked diversions and returns; and 3) determining the activity of located diversions and returns.

Two unexpected challenges were encountered during ground-truthing: 1) determining the status of a diversion or return locations as active or inactive; and 2) determining if a location is permanent or temporary. Observing a pump at a distance, the status as active or inactive is challenging unless the pump is actually running during field observation. To determine the status of a diversion or return, the condition of the

location including the pump, wiring, and piping was examined. In general, if the location appeared to be well maintained and in good condition, the site was assumed to be active. However, if the pump, piping, or wiring, appeared to be in poor condition, the site was assumed to be inactive (Figure 11). Additionally, while traversing across Fabian Tract, two previously identified diversions were found. Piping for these diversions was laid over the top of the levee which surrounds Fabian Tract and appeared to be relatively mobile (Figure 11). The mobility of such locations raises concerns of diversion mobility. For this study, all validated locations were assumed to be permanent.

Figure 11. Images of diversion and return locations, clockwise from the top left corner: active diversion pump; inactive diversion pump depicting cut wires; inactive siphon depicting pipe separations; and temporary diversion, depicting flat piping laid over a levee road.

The ground-truthed DFG and DWR diversion and return locations were combined with the confirmed return locations from LIDAR (Figures 12 and 13). On Fabian tract, with the exception of one predicted return spaced between other predicted returns on the northern edge of Fabian Tract, the predicted returns were valid and located where expected. Most published diversions were valid with the exception of one listed but non-existent diversion, two new permanent locations, and two mobile diversions along the southern region of Fabian Tract. On Staten Island, all predicted returns were valid and no unpredicted returns existed. Additionally, all verified (through Google Earth) published diversion locations and one unpublished diversion location, located through Google Earth, existed.

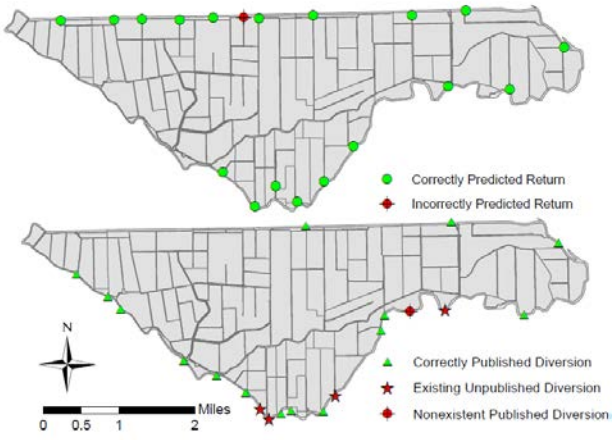

Figure 12. Ground-truthed diversion and return locations on Fabian Tract.

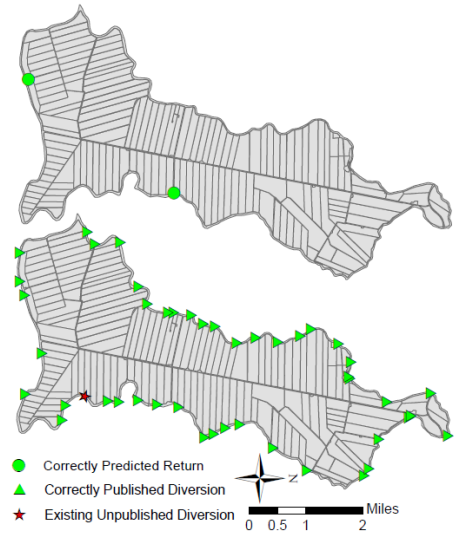

Figure 13. Ground-truthed diversion and return locations on Staten Island.

3.3 Task 3: Model Incorporation

To perform a water budget analysis and estimate the volumes of water diverted to and returned from Fabian Tract and Staten Island, hydrological models were developed and simulations preformed with data from two distinctive water years.

3.3.1 Model Selection

Various models were considered to perform the hydrological analysis; DETAW, IWFM, IDC, MODFLOW, and MF-FMP. The IDC model was selected to simulate the water demands and returns from Fabian Tract and Staten Island based on its capabilities, ease of use, applicability and DWR recommendations. Note, IDC refers to the generic IDC model, and IDC-FT and IDC-SI refer to the IDC models of Fabian Tract and Staten Island respectively.

3.3.2 Development of IDC Inputs

IDC requires input parameters incorporating soil and land-use characteristics as well as meteorological data. Additionally, return flow fractions are specified to account for irrigation non-uniformity and imperfect irrigation efficiency. These parameters are applied to individual elements, which make up subregions in IDC, to calculate irrigation requirements and returns of each subregion.

Fabian Tract and Staten Island were manually divided into subregions, representing fields, levees, ditches, and roads, using Esri ArcGIS. Aquaveo SMS was then used to generate grids on Fabian Tract and Staten Island, representing the developed subregions on Fabian Tract and Staten Island, to be used in the IDC (Figure 14).

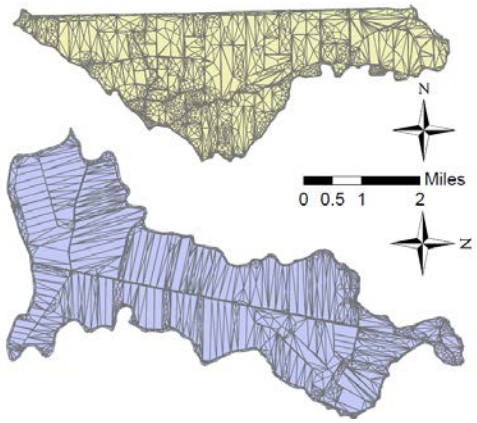

Figure 14. Model area and simulation grid of Fabian Tract (above) and Staten Island (below).

Physical soil properties were applied to each grid element using the technique described in the IDCv4.0 Documentation (IHMD 2011a). The Natural Resources Conservation Service (NRCS) Soil Survey Geographic Database (SSURGO) was used to compile the soil physical properties (Figure 15). Using the NRCS web soil survey (2011), the soil physical properties including the field capacity, total porosity, saturated hydraulic conductivity, and soil hydrologic group were averaged over soil horizons for each soil component. Each component defined soil properties were then averaged for each soil map unit. The defined map units were then intersected with the simulation grid cells. For grid cells

intersecting multiple map units, the physical soil properties were averaged over the area of each grid cell to attain a single value defining each soil property for each element. Arithmetic mean values of the pore size distribution index described by Rawls et al. (1982) were assigned to match the dominant soil textures. Additionally, the wilting point for each cell was set to zero.

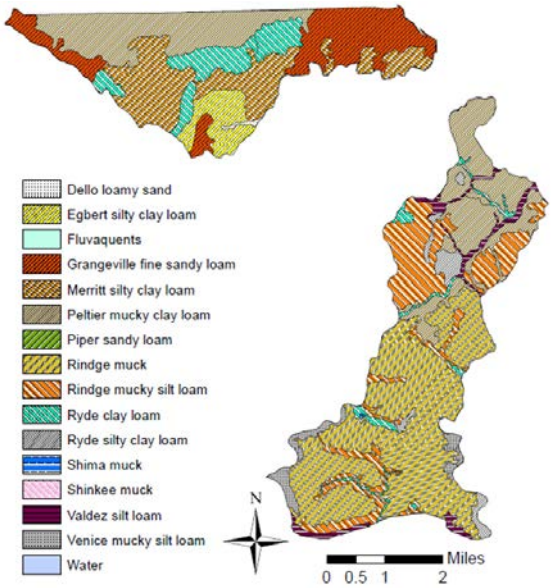

Figure 15. Soil types present on Fabian Tract (above) and Staten Island (below).

For modeling purposes, land-use was divided into four categories: 1) non-ponded, including grain, cotton, sugar beets, corn, dry beans, safflower, alfalfa, pasture, tomatoes, cucurbits, onions and garlic, almond and pistachios, subtropical, fallow and idle, other deciduous, other truck and other field land-use types; 2) ponded, including rice and refuge land-use types; 3) urban, including developed areas; and 4) native and riparian vegetation. Most of Fabian Tract is designated as “field.” “Field” areas were assigned land-use values based on the land-use data from the National Agricultural Statistics Service (USDA 2011), which provided a GIS map of Delta land-use for 2007 and 2010. However, elements designated as “road” were assigned to be 90% developed and 10% idle and fallow; elements designated as “gravel road” were assigned to be 60% developed and 40% idle and fallow; elements designated as “levee” were assigned to be 15% riparian, 60% native vegetation, and 25% developed; and elements designated as “ditches” were assigned to be 50% riparian and 50% idle and fallow. Values for areas designated as “road”, “levee”, or “ditches” were based on visual observations made while ground truthing. Regions designated as “open water” were determined to be insignificant (less than 0.05% of the total area) and were incorporated into the riparian land-use category. From intersecting the National Agricultural Statistics land-use map with the “field” elements and assigning land-use values to all other grid elements based on their designation, the primary land-use types on Fabian Tract were determined to be corn and alfalfa whereas the primary land-use type on Staten Island was determined to be corn (Figures 16 and 17).

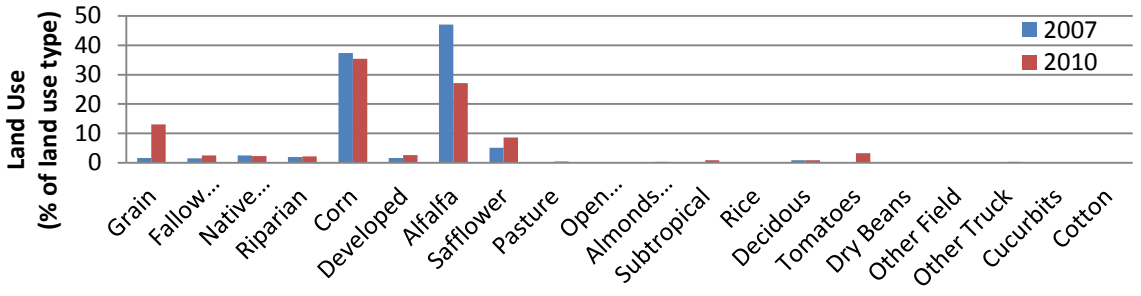

Figure 16. Land-use on Fabian Tract.

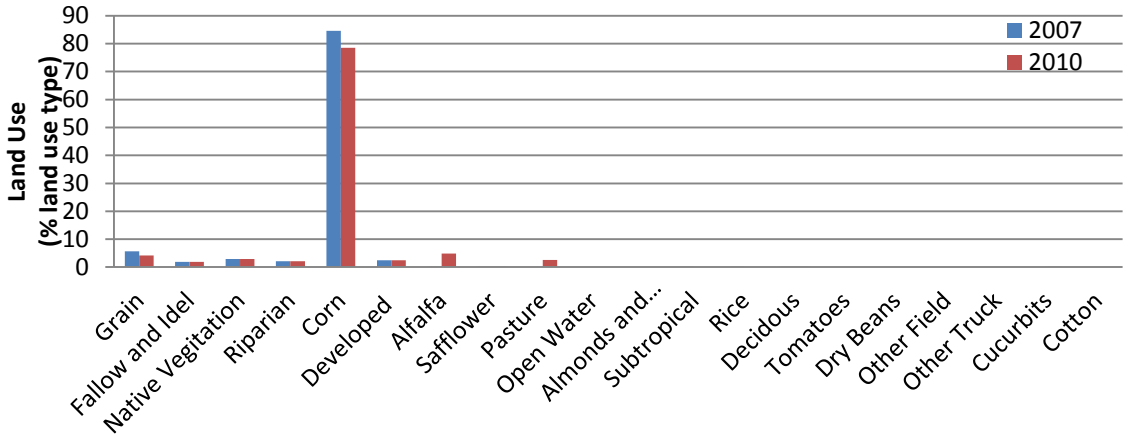

Figure 17. Land-use on Staten Island.

In "Example 2: A Real-World Application" of the IWFM Theoretical Documentation, ET data in a northern region of the Central Valley of California is examined by the Integrated Hydrological Models Development Unit (IHMD 2011a). In the sample problem, to avoid problems matching ET data from the DWR with constant land-use areas, ET data for each land-use type at each grid cell was obtained from the Calsim 3.0 project on a monthly basis. In this case, ET changed from month to month, but monthly values remained constant on an annual basis (IHMD 2011a). Since Fabian Tract and Staten Island are in the Central Valley of California, the ET values used for the "Real-World Application" were assumed to be valid for the same agricultural crops within the model area and were applied.

The California Irrigation Management Information System (CIMIS) was used to locate different meteorological stations within the Delta. Using Thiessen polygons and considering topographical variations, meteorological data from the Tracy Weather Station were selected to be used for IDC-FT whereas meteorological data from the Twitchell Weather Station were selected to be used for IDC-SI. To have a realistic initial soil-water mixture storage for each model year based on irrigation and precipitation prior to the model run, historical meteorological data were input into IDC-FT and IDC-SI allowing for model spin up periods. Meteorological data for a dry year, 2007, and for a wet year, 2010, were then used for each model simulation respectively (Figures 18 and 19). Here, model years refer to water years (e.g., October 1, 2006 through September

30, 2007 is water year 2007). The precipitation trends between the meteorological stations remains the same, but the scale of the precipitation events changes between the stations.

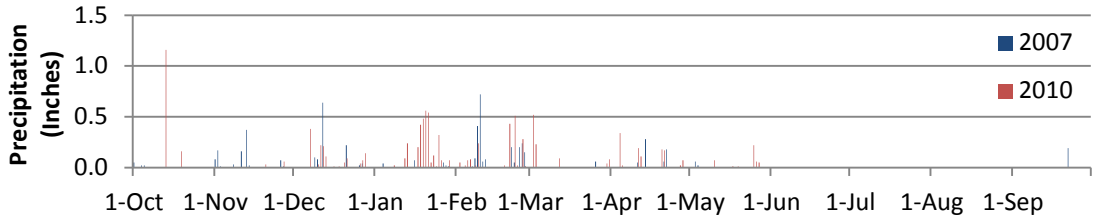

Figure 18. Daily precipitation at the Tracy meteorological Station.

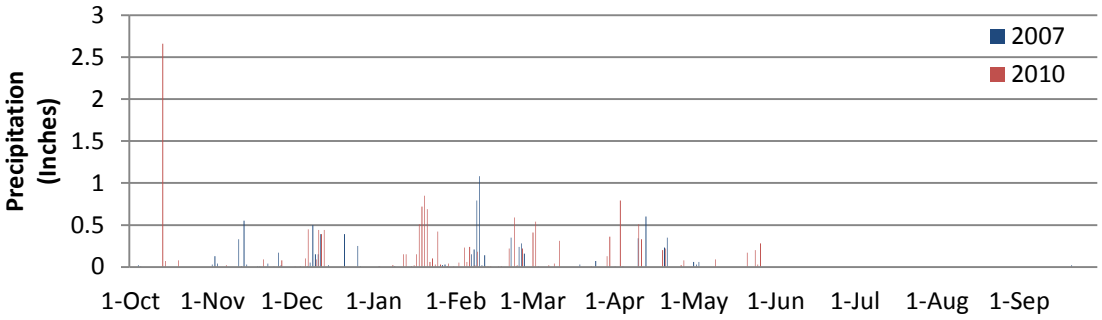

Figure 19. Daily Precipitation at the Twitchell Meteorological Station.

Using the method described in the ArcGIS Analysis section, diversion and return locations were determined for Fabian Tract and Staten Island subregions based on their drainage patterns. Combining subregions based on their allocated diversion and return locations, diversion and return watersheds were delineated (Figures 20 and 21). Diversion watersheds represent the total area fed by a diversion source whereas return watersheds represent the total area draining to a return sink.

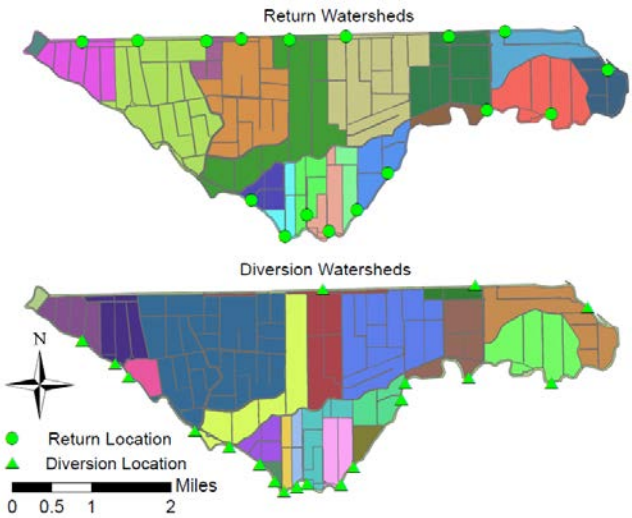

Figure 20. Fabian Tract diversion and return subregion allocation.

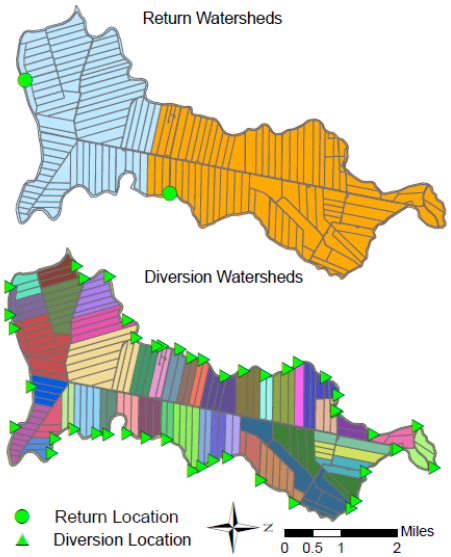

Figure 21. Staten Island diversion and return subregion allocation.

3.3.3 IDC-FT Model Calibration

To test the performance of IDC-FT during dry and wet conditions, model runs were initially made using precipitation data for 2007 and 2010, input parameters determined from the Natural Resources Conservation Service's (NRCS) Soil Survey Geographic Database (SSURGO), and land use data for 2007 and 2010 (Figures 22 and 23). Diversion and return trends for 2007 and 2010 were similar, however the volume and timing of water diversions between the water years varied. For 2007 and 2010, large spikes in diverted water were observed, signaling that the root zone water content reached a critical state requiring diverted water to recharge the root zone water content. These large spikes were then followed by smaller slightly offset spikes in returned water. As expected, more diverted water was required for the dry year, 2007, than for the wet year, 2010. However, for 2007 water was shown to be continuously applied to ponded crops during the growing season, raising concerns of the model validity (Figure 21). Contributing to concern, dividing the total annual diverted water by the area of Fabian Tract, the diverted water demands were significantly larger than expected (Appendix C). By comparison with other water use estimates, diverted water requirements determined by IDC-FT for 2007 and 2010 were determined to be unrealistically high (DWR 2012; Medellin-Azuara 2012). Ponded crops for 2007 and 2010 were incorrectly modeled as having a continuous supply of diverted water in addition to the peak withdrawals from the depletion of water in the root zone. This led to unrealistically high applied water demands for ponded crops.

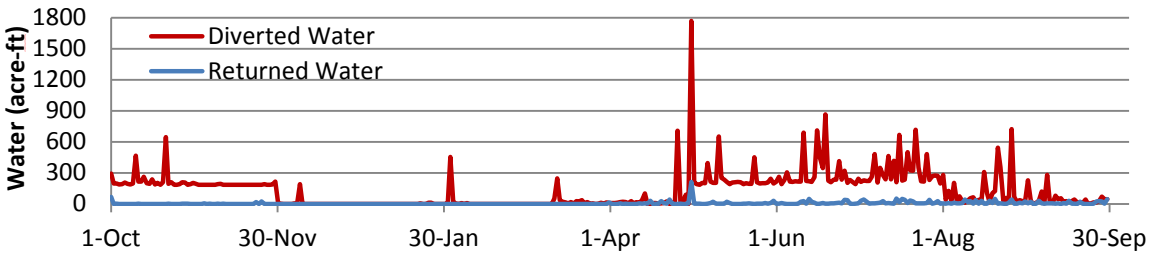

Figure 22. 2007, daily total daily diverted and returned water on Fabian Tract.

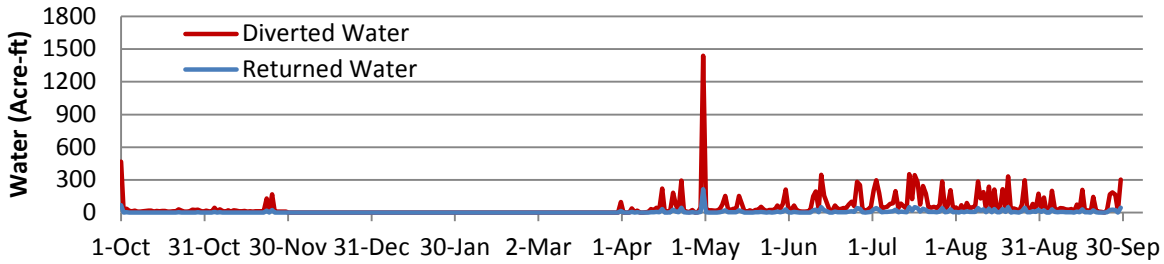

Figure 23. 2010, total daily diverted and returned water on Fabian Tract.

Applied water demands for non-ponded crops are insensitive to changes in the saturated hydraulic conductivity; however applied water demands for ponded crops are sensitive to changes in saturated hydraulic conductivity (Williams 2004; Dogrul et al. 2011). In the report Root Zone Moisture Routing and Water Demand Calculations in the Context of Integrated Hydrology hydraulic conductivities ranging from 0.01 to 0.1 µm/s

were used to attain realistic applied water demands from ponded crops with IDC (Dogrul et al. 2011). For this reason, IDC-FT runs were made for 2007 using saturated hydraulic conductivity values ranging from 0.01 to 0.1 µm/s for all model elements with ponded crops. The error encountered in applied water demand for ponded crops was removed through this approach and the applied water demands from ponded crops appeared reasonable for the entire range of saturated hydraulic conductivity values used.

For modeling purposes, a mid-range saturated hydraulic conductivity (K) of 0.05 µm/s was applied to all IDC elements with ponded crops. Similar to the initial IDC-FT simulation, large spikes in diverted water were observed followed by slightly offset spikes in returned water (Figures 24 and 25). However, water was not shown to be continuously diverted to ponded crops during growing seasons and the applied water demands were significantly reduced, although still larger than expected.

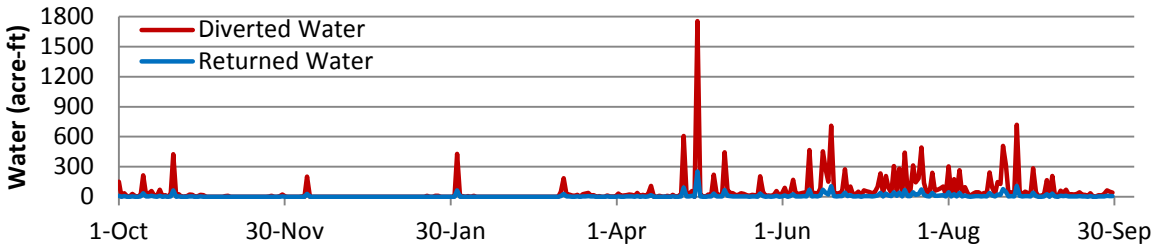

Figure 24. 2007, total daily diverted and returned water on Fabian, K= 0.05 µm/s for all ponded elements.

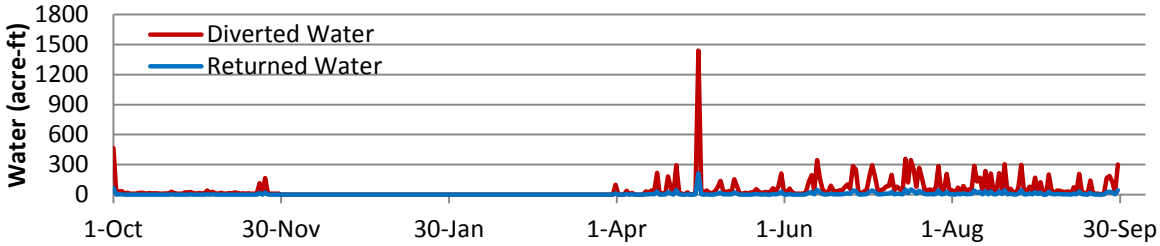

Figure 25. 2010, total daily diverted and returned water, K=0.05 µm/s for all ponded elements.

Owen and Nance (1962) and others have suggested that ground water seeps from neighboring Delta island channels and is a function of the soil characteristics as well as hydraulic gradient which varies throughout the Delta. However, historically the California Department of Water Resources has assumed a uniform seepage rate across the Delta of 0.025 inches per foot rooting depth per month (Kadir 2012). For consistency, this value was applied to IDC-FT (Figures 26 and 27). The general trends remained the same; large spikes in diverted water were followed by smaller slightly offset spikes in returned water. However, the irrigation period was significantly reduced and the initial large spikes of diverted water at the beginning of the irrigation period were eliminated, leading to significant reductions in diverted water that appear valid.

IDC-FT parameters developed through the calibration process described above were applied to IDC-SI.

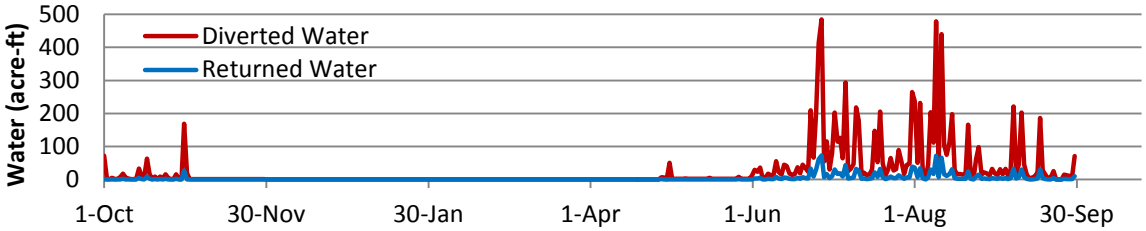

Figure 26. 2007, total daily diverted and returned water, K=0.05 µm/s for all ponded elements and assuming a constant seepage rate onto Fabian Tract of 0.025 inches per foot rooting depth per month.

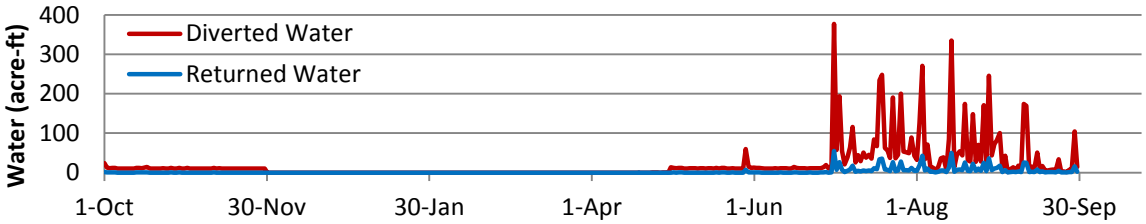

Figure 27. 2010, total daily diverted and returned water, K=0.05 µm/s for all ponded elements and assuming a constant seepage rate onto Fabian Tract of 0.025 inches per foot rooting depth per month.

3.4 Task 4: Prediction of Water Quality of Return Flows

Agricultural discharges into streams can affect stream water quality. However, the scale of these effects is difficult to determine. To develop a correlation between the water quality of Delta streams and the water quality of return flows, water quality data from numerous water quality monitoring studies conducted in California, with most taking place in the Sacramento-San Joaquin Delta, were collected (Figure 28) (DWR 1991; Hoffman 2010; Marvin Jung and Associates Inc. 2000; Templin and Cherry 1997).

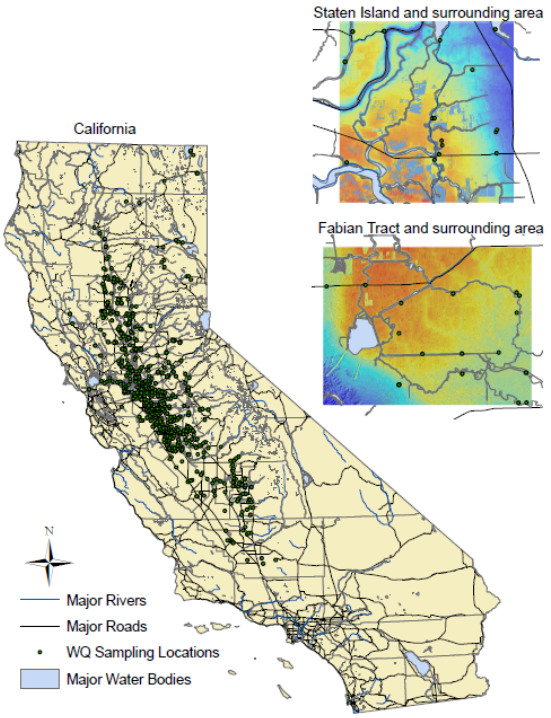

Figure 28. Water quality sampling stations within California (CV RDC 2011).

4 Results and Discussion

Diversion and return locations from existing data and ground-truthing were coupled with IDC to model diversion and return flows on Fabian Tract and Staten Island. Return flow patterns were then compared with existing water quality data to examine correlations between return flows and the effects of return flows on in-Delta streams. In the following sections, results of the Delta island topography analysis, IDC-FT and IDC-SI simulations, and Delta water quality correlation are presented and discussed.

4.1 Delta Island Topography

A combination of LIDAR DEM and existing diversion and return data was collected and analyzed to make DICU predictions in a non-invasive manner. The validity of documented and predicted locations was ground-truthed. The results on Fabian Tract were then compared to existing DICU model diversion and return locations.

Diversion locations were predicted by combining the DFG and DWR data and examining the status of each location in associated metadata. All documented locations were found to exist on Fabian Tract with the exception of one documented but non-existent location on the south-east bank (Figure 29). On Staten Island, all documented locations were found to be present (Figure 30). However, during ground-truthing four undocumented diversions were found on Fabian Tract and one undocumented diversion was found on Staten Island. On Fabian Tract, two of these diversions appeared to be permanent, while the other two diversions appeared to be mobile, suggesting that they may be temporary. The diversion found on Staten Island appeared to be permanent. The undocumented diversions are near existing documented diversions. For this reason, the errors in diversion locations are not expected to significantly affect the diversion patterns for Fabian Tract or Staten Island.

The predicted return locations were found to be correct with the exception of a predicted return on the north side of Fabian Tract (Figures 29 and 30). The incorrectly predicted return is spaced closely between two other return locations suggesting that the return patterns from Fabian Tract would not be significantly affected by this error.

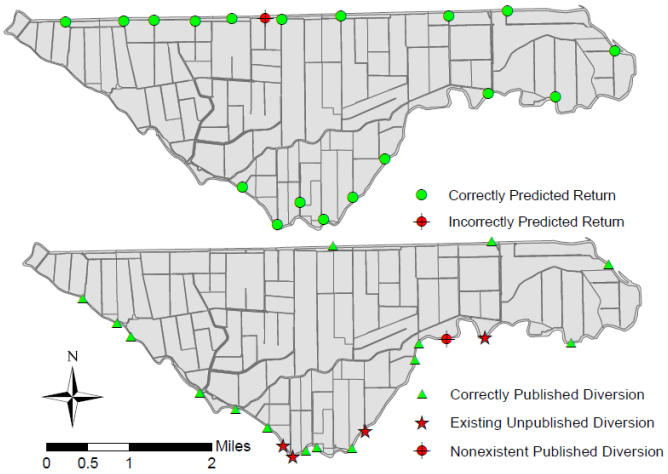

Figure 29. Comparison of expected diversion and return locations to ground-truthed results.

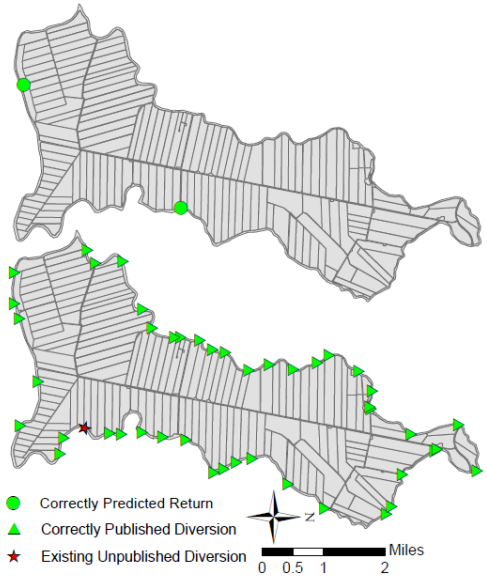

Figure 30. Ground-truthed diversion and return locations on Staten Island.

Significant differences in the location and number of diversions and returns exist between the ground-truthed data and those listed in the Sacramento-San Joaquin Delta Atlas (1995) as well as the current DICU model (Table 2; Figures 31-34). On Fabian Tract, the ground-truthed returns and diversions match fairly well to those listed in the California Water Atlas. However, the California Water Atlas lists a greater number of diversions from the North side of Fabian Tract than was observed during ground-truthing. Although the number of diversions and returns in the current DICU model varies from those observed during ground-truthing, the general pattern of diversion and return locations on Fabian Tract is similar. Most existing diversions observed and those modeled in the current DICU model are on the south side of Fabian Tract. Additionally, most existing returns observed and those modeled in the current DICU model are on the north side of Fabian Tract. Terrain, land gradient, and drainage networks probably make this pattern enduring.

The diversion and return locations listed in the California Water Atlas match fairly well to the ground-truthed locations on Staten Island, however the locations and quantity of diversion and return locations listed in the current DICU model poorly match the ground-truthed locations. The current DICU model lists the same number of return locations observed during ground-truthing on Staten Island, two, however the location of these returns in the DICU model do not match the locations observed during ground-truthing. Furthermore, the current DICU model lists only 11 diversions, whereas 46 diversions were observed during ground-truthing. Additionally, not the entire DICU diversion locations match with diversion locations observed during ground truthing.

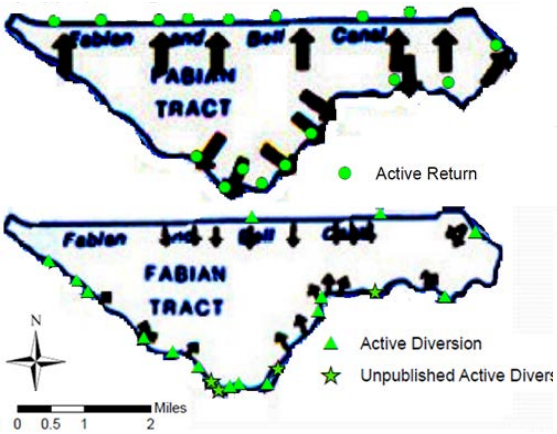

Figure 31. Fabian Tract ground-truthed diversions and returns vs. Sacramento-San Joaquin Delta Atlas.

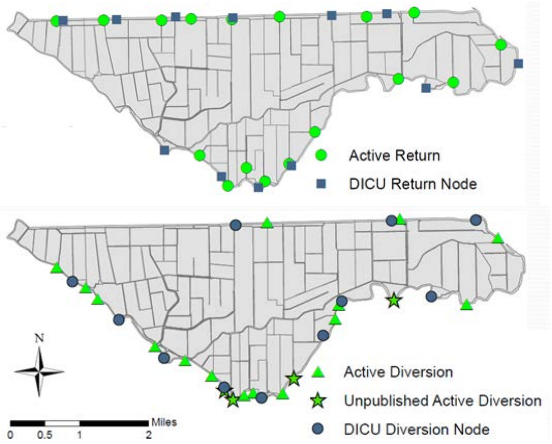

Figure 32. Fabian Tract ground-truthed diversions and returns vs. Sacramento-San Joaquin Delta Atlas.

Figure 33. Staten Island ground-truthed diversions and returns vs. Sacramento-San Joaquin Delta Atlas.

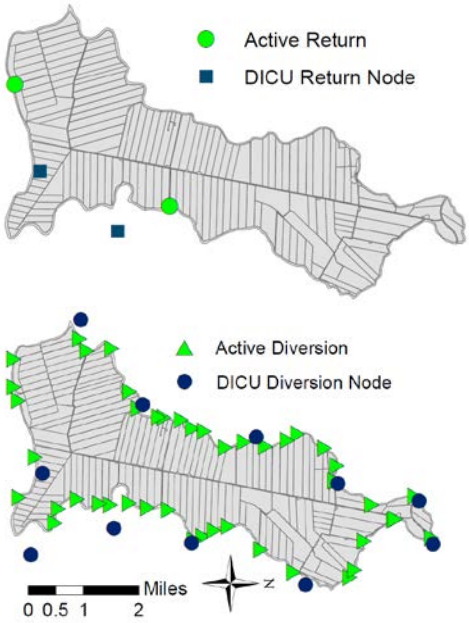

Figure 34. Staten *Island ground-truthed* diversions and returns vs. Sacramento-San Joaquin Delta Atlas.

Table 2. Summary of diversion and return locations (near matches in parenthesis).

	Fabian Tract		Staten Island	
	Diversions	**Returns**	**Diversions**	**Returns**
Ground-Truthed	19	17	46	2
Water Atlas	13 (10)	13 (10)	45 (40)	2 (1)
DICU	12 (10)	11 (10	11 (9)	2 (0)

4.2 IDC-FT and IDC-SI Model Results

IDC models were developed and integrated with ArcGIS data along with cropping and irrigation schemes to perform a water budget analysis of Fabian Tract and Staten Island (Figure 35). The daily volume of water diverted and returned from each ground-truthed location was estimated (Figures 33 and 34, Appendix E). The volume and timing of water diverted and returned at each location varied and is correlated to the total daily volume of water returned; however, the volume of water returned at a given location is not necessarily directly correlated to the volume of water diverted from any given diversion. For example, a large spike in withdrawn water at a single location may correlate to spikes in returned water at multiple locations.

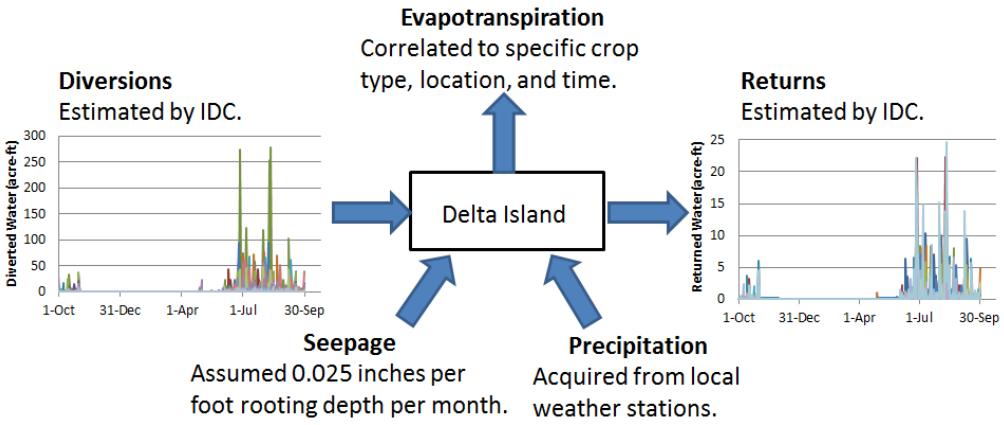

Figure 35. Summary table of water budget analysis.

The initial IDC models assumed no limiting rates for water diversion or return, allowing unrealistic volumes of water to be modeled as diverted or returned on any given day. To account for diversion and return limits, maximum flow rate capacities, determined from pump unit use coefficients, pump horsepower ratings, and given flow rate capacities, were applied at each location (Figures 36-38, Appendix F). For unrated locations, rate capacities were assumed to be the average of the known pump or siphon capacities of a similar size. For diversion siphons or pump diversions of an unknown size, the flow rate capacity was assumed to be enough to meet annual demand.

Applying flow rate capacities at each location while maintaining the total volume of water modeled by IDC as diverted and returned significantly flattens and broadens the diversion and return peaks. The volume and timing of water diverted and returned at each location still varies with peaks in diverted water followed by smaller offset peaks in returned water. However, flow rate limitations reduce peak diversion and return rates (Figures 39-41 and Appendix E). To maintain the same volume of water being diverted or returned, the duration of peak withdrawals and returns is increased, allowing smaller daily rates of diverted and returned water to meet demands.

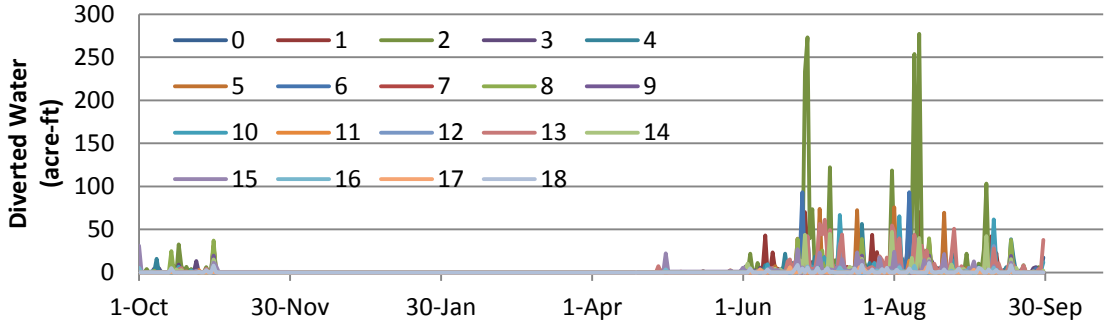

Figure 36. 2007, daily diverted water on Fabian Tract from ground-truthed diversion locations.

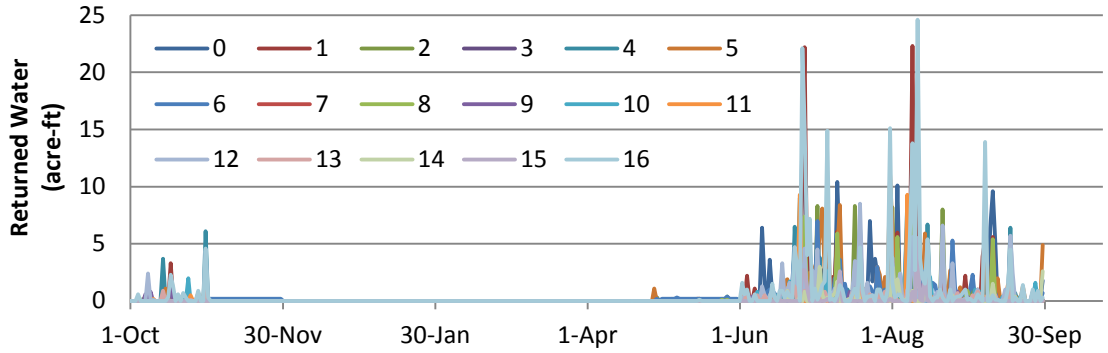

Figure 37. 2007, daily returned water on Fabian Tract from ground-truthed return locations.

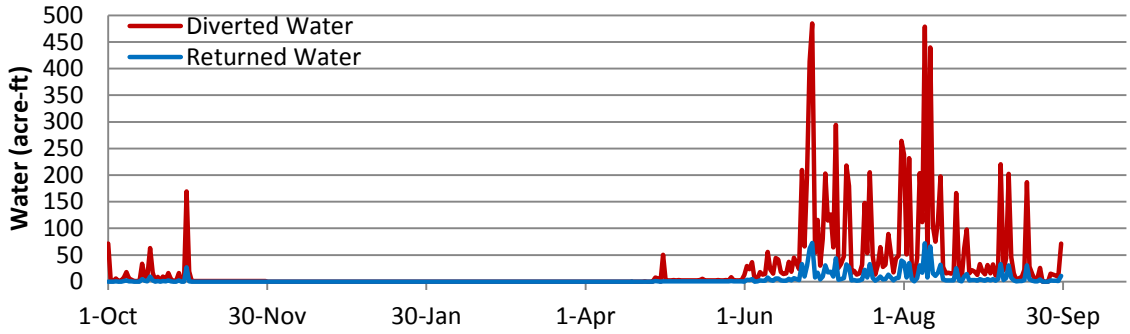

Figure 38. 2007, total daily diverted and returned water using a saturated hydraulic conductivity of 0.05 µm/s for all ponded elements and assuming a constant seepage rate onto Fabian Tract of 0.025 inches per foot rooting depth per month.

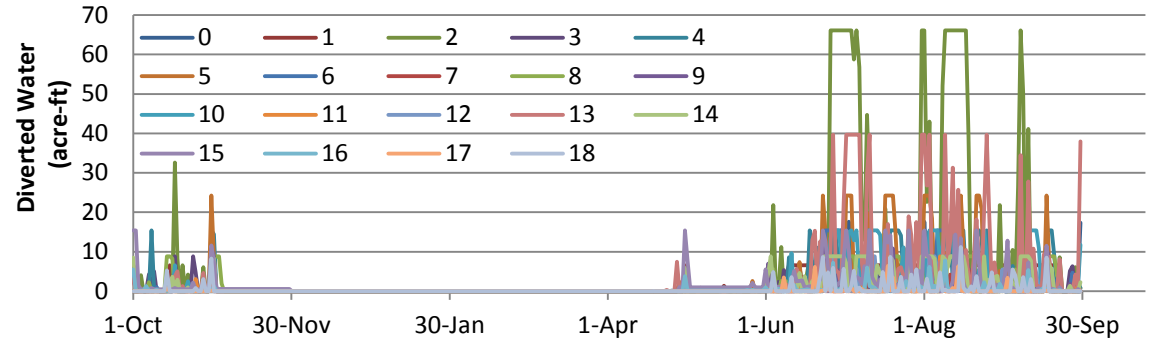

Figure 39. 2007, daily diverted water on Fabian Tract from ground-truthed diversion locations with limits applied to the diversion rate.

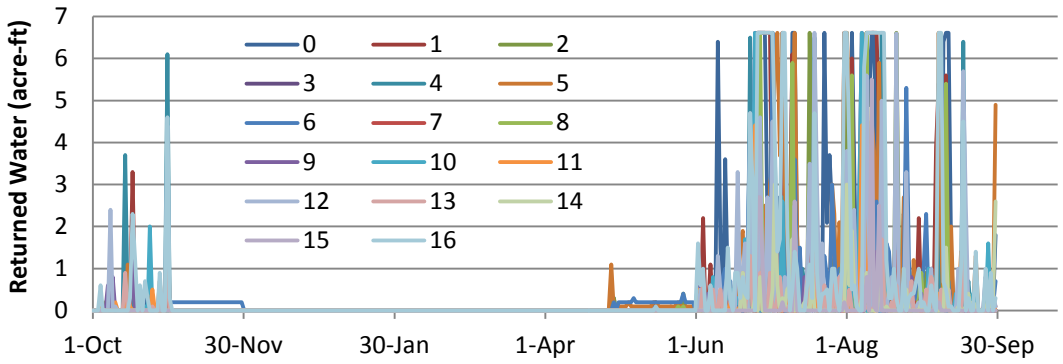

Figure 40. 2007, daily returned water on Fabian Tract from ground-truthed return locations with limits applied to the return rate.

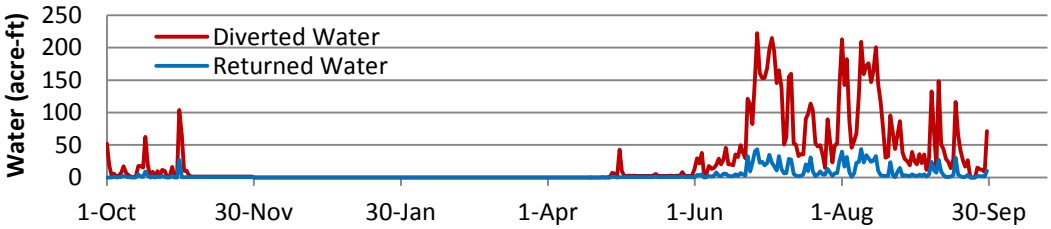

Figure 41. 2007, total daily diverted and returned water using a saturated hydraulic conductivity of 0.05 µm/s for all ponded elements, assuming a constant seepage rate onto Fabian Tract of 0.025 inches per foot rooting depth per month, and applying diversion and return rate limits.

To visually examine the volume of water diverted and returned from Fabian Tract and Staten Island, IDC-FT and IDC-SI results were integrated into ArcGIS (Figures 42-43). On Fabian Tract in 2007 and 2010, most diverted water on Fabian Tract was withdrawn from the southern side of the island, and most agricultural runoff was returned on the northern side of the island. On Staten Island in 2007 and 2010, water was fairly evenly diverted onto the island and returned from the two given return locations.

The diversion and return patterns of Staten Island significantly differ from those observed on Fabian Tract. In part, this difference is the result of the level of subsidence observed on the two Islands. Fabian Tract is less subsided, making siphoning difficult or infeasible for some areas. Additionally, the locations where siphoning is possible are generally at the lowest point on the island, thus siphoned water at these locations would need to be piped, and possibly pumped, uphill to irrigate crops. For this reason, water is generally pumped onto the highest parts of the island and then allowed to drain to the lower regions for irrigation and return. On the other hand, Staten Island is so subsided that water can easily be siphoned onto the island at any location. The water then drains to a central ditch which runs the entire length of the island to return water. As a result, many more diversion locations are on Staten Island than on Fabian Tract, but Fabian Tract has more returns than Staten Island.

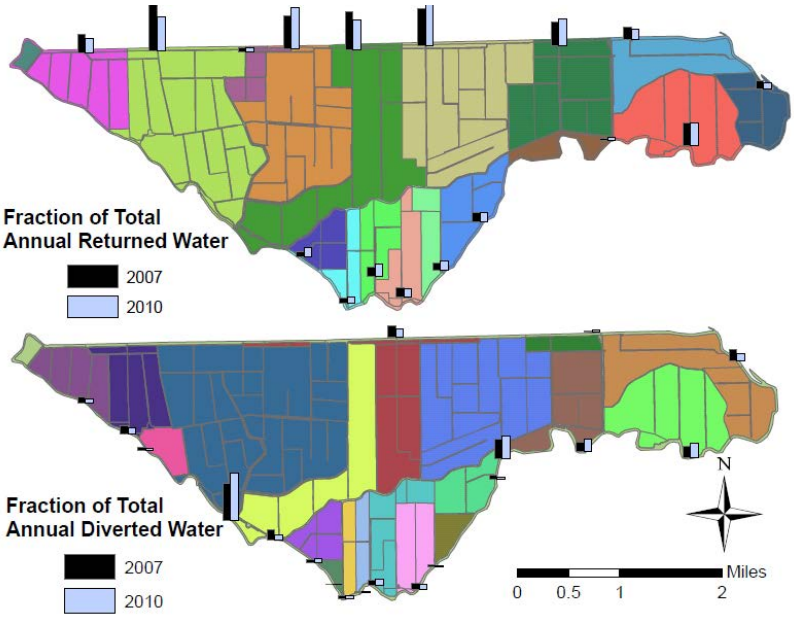

Figure 42. Fabian Tract diversion and return patterns, showing the annual fraction of total water diverted and returned at a given location per watershed for 2007 and 2010.

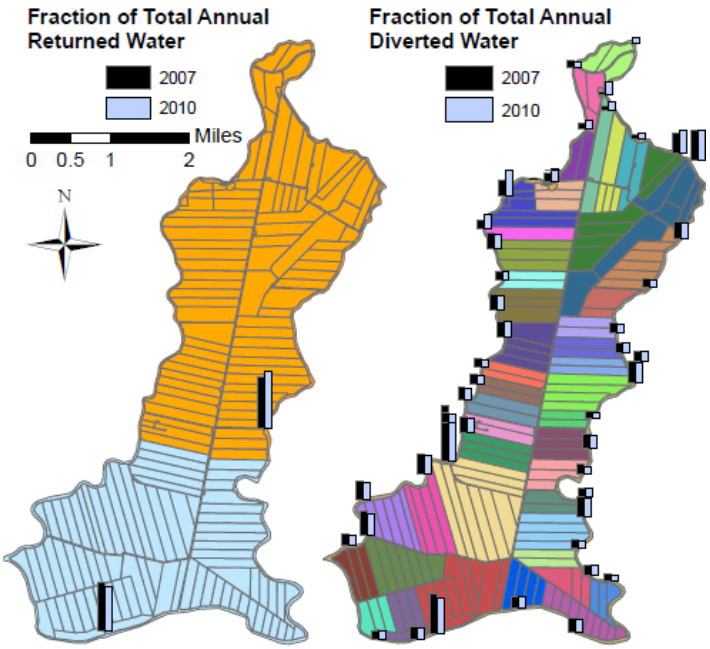

Figure 43. Staten Island diversion and return patterns, showing the annual fraction of total water diverted and returned at a given location per watershed for 2007 and 2010.

4.2.1 Existing Model Comparisons

Post processed model results of diversion, return, and seepage values for Fabian Tract and Staten Island were obtained from the current DWR DICU model and a recently developed DWR model in DETAW (Liang 2012). These post processed results, referred to as Post-DICU and Post DETAW respectively, were then used for comparison with IDC-FT and IDC-SI results.

The annual fraction of water routed through each Fabian Tract and Staten Island DICU node was combined with GIS analysis to compare to IDC-FT and IDC-SI results (Figures 44 and 45). The IDC model trends of diverted water on Fabian Tract and Staten Island match the Post-DICU trends fairly well. On Fabian Tract, most water is withdrawn from the southern side of the island, whereas on Staten Island a fairly even proportion of water is withdrawn from all sides of the island. However, the IDC model trends of returned water on Fabian Tract and Staten Island poorly match the Post-DICU trends. IDC-FT shows most water returned to the northern side of Fabian Tract whereas post-DICU results indicate that most agricultural runoff is returned back to the southern side of the island. Additionally, IDC-SI shows a relatively even split of returned water at the two known return locations on Staten Island, where as the post-DICU results indicate that the majority of water is returned at the southernmost return on the island. From the topography analysis of Fabian Tract and Staten Island using LIDAR DEM data as previously described, Fabian Tract slopes downwardly in a north-west direction whereas Staten Island is fairly evenly subsided. Based on the general slopes of the islands and the locations of ground-truthed returns, post-DICU results are expected to be less accurate than the IDC model results.

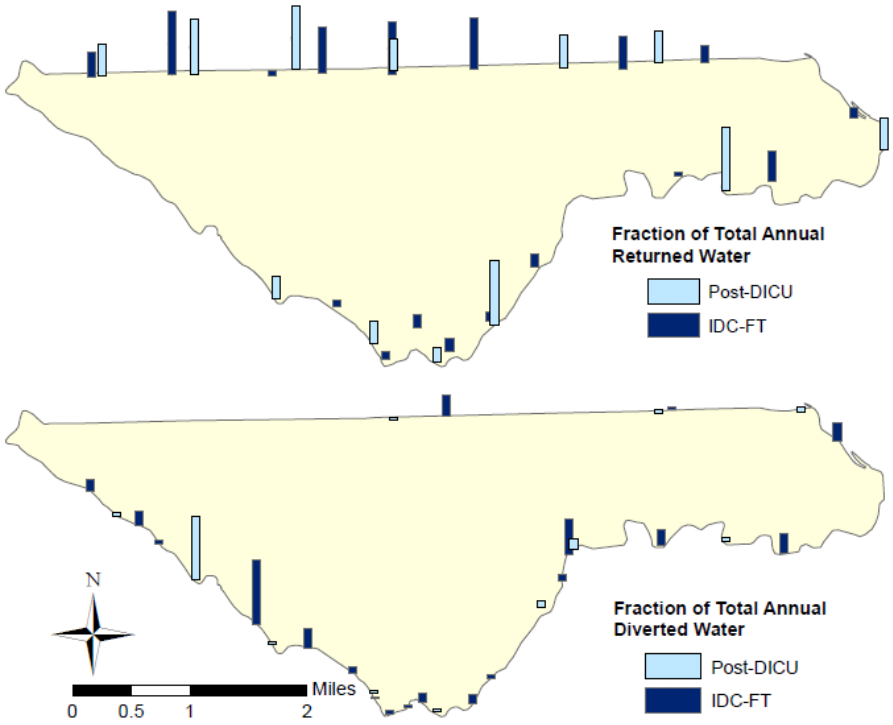

Figure 44. Comparison of IDC-FT and Post-DICU results for 2007, showing the total annual fraction of water diverted or returned at respective locations.

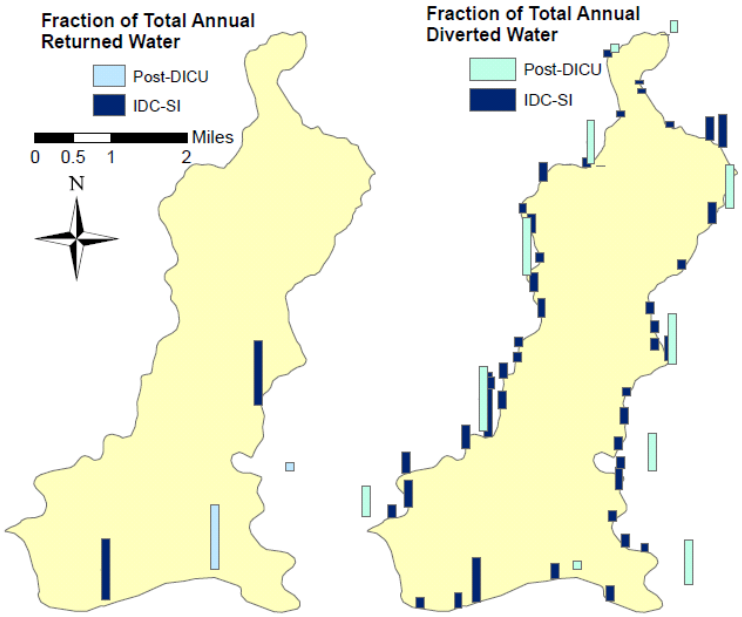

Figure 45. Comparison of IDC-SI and Post-DICU results for 2007, showing the total annual fraction of water diverted or returned at respective locations. Note: diversion and return locations are georeferenced and may not necessarily be located on Staten Island within the model.

Net channel depletion, diverted water, returned water, and seepage values for the IDC models were also compared to Post-DICU and Post-DETAW results. Since Post-DICU, Post-DETAW, and IDC-FT areas are of different size, volume units were converted into unit depths (acre-feet/acre).

IDC-FT annual estimates of net channel depletion, diverted water, and seepage fall between Post-DICU and POST-DETAW estimates, however the return volume is lower (Figure 46). Post-DICU and Post-DETAW models use averaged precipitation values for the entire Delta, whereas the IDC-FT and IDC-SI models use values precipitation values from their nearest meteorological stations. Precipitation values vary throughout the Delta and significantly affect model results; these variations may explain observed differences of annual returned water.

General trends of net channel depletion and diverted water on Fabian Tract remain the same between the models, with most water estimated to be diverted during the peak growing season, May through September, as expected (Figures 47 and 48). However, the volumes and timing of net channel depletion and diverted water vary between the models. Post-DICU and Post-DETAW both divert water earlier in the agricultural season than IDC-FT and Post-DICU applies less water than IDFT and Post-DETAW and the end of the agricultural season. Additionally, post-DICU and post-DETAW divert water during winter months which can affect returned water volumes during these months. This may be evident in the trend as the trends and volumes of returned vary between models (Figure 49). Post-DICU and Post-DETAW show a trend in peak return discharges offset from the peak growing season, which is not shown by IDC-FT. This is likely a result of using different precipitation datasets.

The IDC-FT and Post-DICU seepage values remain fairly constant throughout 2007, with an exception in February with the Post-DICU results (Figure 50). This may be expected since the hydraulic gradient between Delta islands and their neighboring channels generally does not change significantly seasonally. However, the Post-DETAW results show seasonal seepage variations.

IDC-SI annual estimates of net channel depletion and diverted water match the Post-DICU and POST-DETAW estimates fairly well, however the IDC-SI return volume and seepage estimates are lower (Figure 51). Here the difference in the return volumes may be the result of varying seepage and precipitation values. The seepage rate, which is assumed to be the same between IDC-SI, DICU, and DETAW, is a function of crop rooting depth. If the models were to use different types of crops during the same water year, different seepage volumes of water would be available for consumption (ET) according to each respective model. This may explain the observed difference in seepage rates. The same general trends of net channel depletion and diverted water observed on Fabian Tract are also observed on Staten Island (Figures 52 and 53). Again, the general trends of returned water and seepage observed on Fabian Tract are also observed with Staten Island. However the return and seepage values of the post-DICU and post-DETAW results significantly exceed the IDC-SI model estimates (Figures 54 and 55).

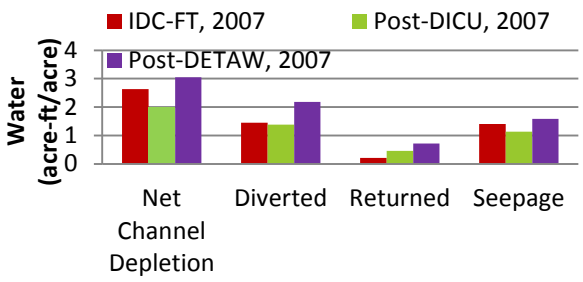

Figure 46. Model comparison of annual net channel depletion, diverted water, returned water and seepage on Fabian Tract.

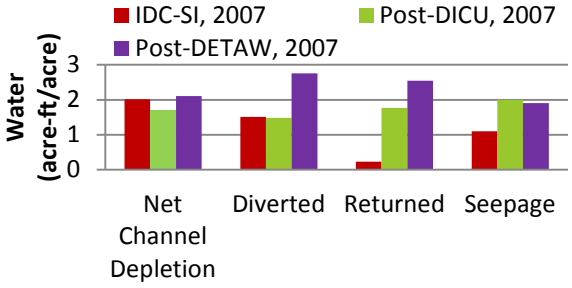

Figure 51. Model comparison of annual net channel depletion, diverted water, returned water and seepage on Staten Island.

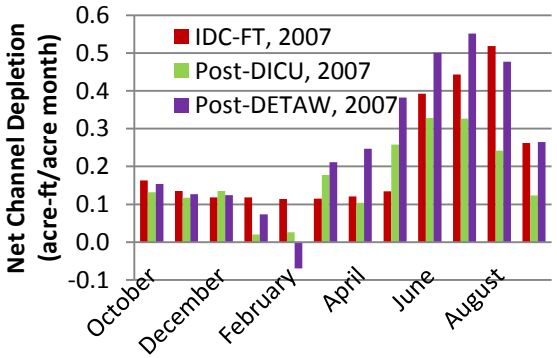

Figure 47. Model comparison of monthly net channel depletion on Fabian Tract

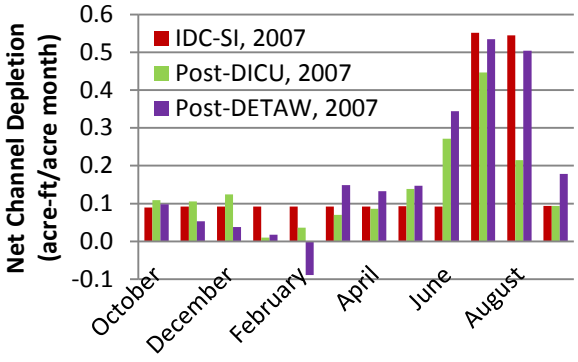

Figure 52. Model comparison of monthly net channel depletion on Staten Island.

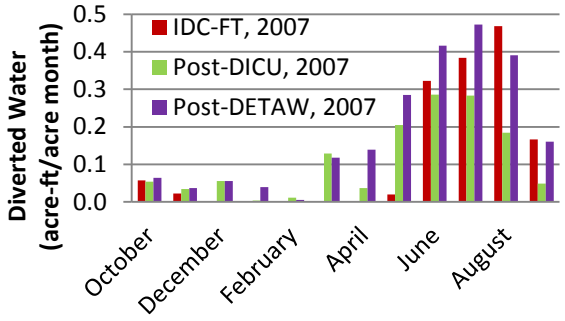

Figure 48. Model comparison of monthly diverted water on Fabian Tract.

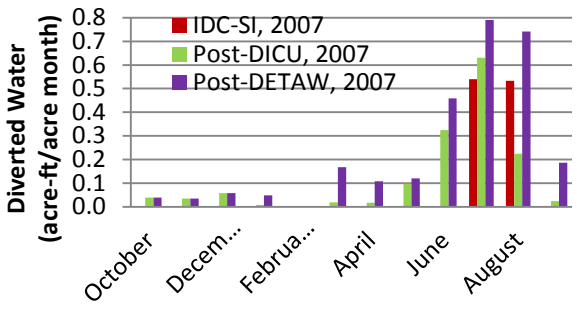

Figure 53. Model comparison of monthly diverted water on Staten Island.

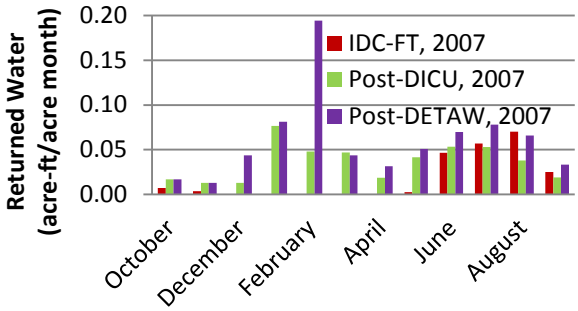

Figure 49. Model comparison of monthly returned water on Fabian Tract.

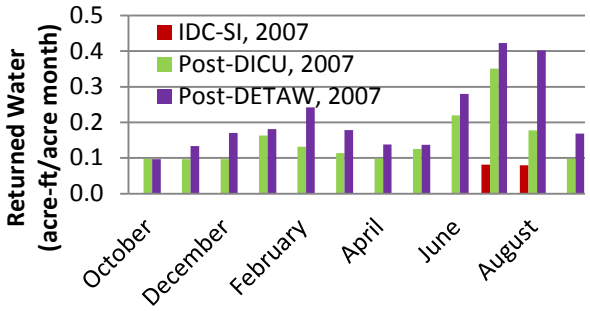

Figure 54. Model comparison of monthly returned water on Staten Island.

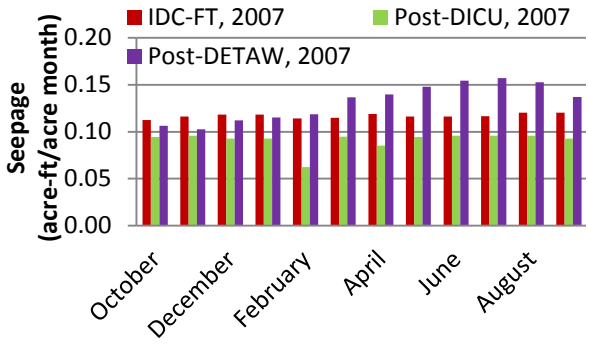

Figure 50. Model comparison of monthly seepage on Fabian Tract.

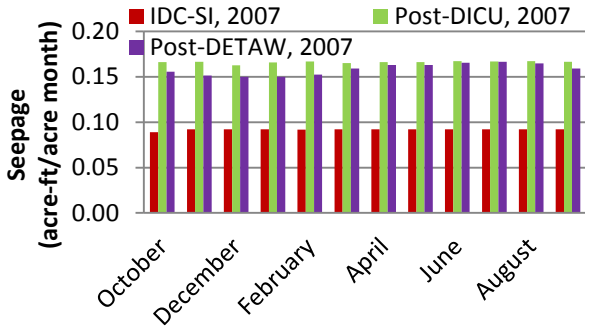

Figure 55. Model comparison of monthly seepage on Staten Island.

4.2.2 Historical Comparison

During 1960 Owen and Nance conducted a study of Twitchel Island, monitoring surface inflow, drain discharge, precipitation, changes in soil moisture content, weather data, and cropping patterns and methods. IDC model runs were not made for 1960, but were performed for both a wet and dry water years, the Owen and Nance values are to be compared to the IDC 2007 and 2010 model results for both Fabian Tract and Staten Island. Since the Islands are of a different size, unit depth of water will be used in this comparison.

The annual volume of diverted water reported by Owen and Nance matches nicely with the IDC-FT and IDC-SI results, but differences in net channel depletions,

returns, and seepage exist (Figure 56). The most significant difference in estimated values and those reported by Owen and Nance exist between returned water. This difference may be the result the many parameters affecting agricultural practices such as soil characteristics, irrigation efficiency, precipitation, and leaching practices.

Trends of net channel depletions and diverted water remain the same between estimated values and those reported by Owen and Nance, with net channel depletions and diversions increasing during the summer and reducing during the winter (Figures 57 and 58). However, Owen and Nance report water being diverted during the winter months whereas no water is estimated as being diverted during the winter by the IDC model. This difference may be the result of leaching practices which are not accounted for, but may be added, in the IDC models.

Trends of returned water vary between estimated values and those reported by Owen and Nance (Figure 59). Since Owen and Nance report water being diverted in the winter, runoff and therefore returned water would be expected during the winter as reported by Owen and Nance. The IDC model does not report diverted water during the winter, thus the only water returned would be that resulting from the overland flow of precipitation and through seepage. If the field capacity is not reached from precipitation and seepage alone, no overland flow would occur and thus no water would need to be returned during the winter, as estimated by the IDC model runs.

Seepage estimates vary from those reported by Owen and Nance; however the rate at which seepage occurs remains fairly constant, as expected (Figure 60). Owen and Nance report a greater rate of seepage than estimated by the IDC models. This rate is a function of the hydraulic gradient and soil characteristics which vary among Delta Islands.

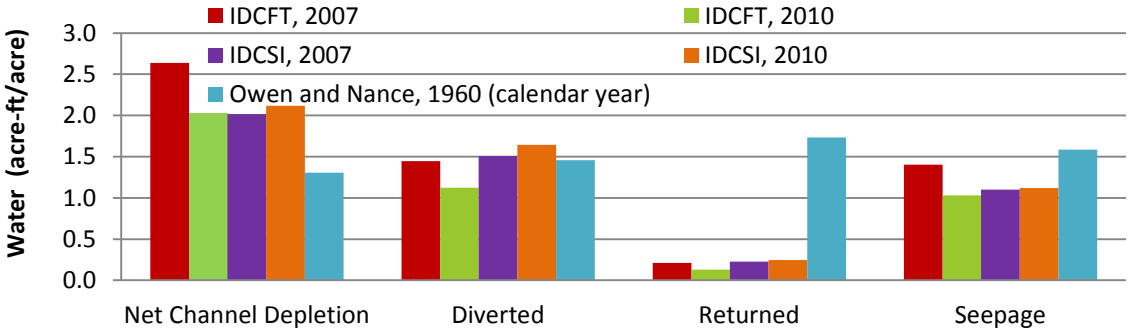

Figure 56. Comparison of annual net channel depletion, diversion, returned, and seepage estimates to values reported by Owen and Nance (1962).

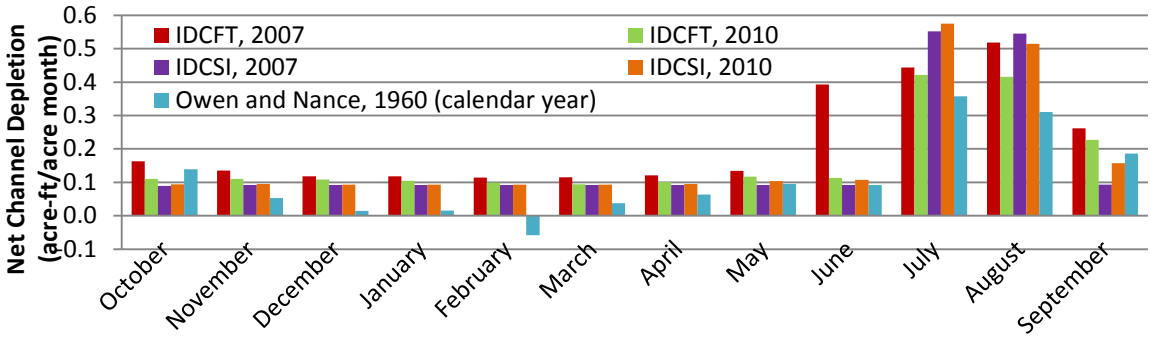

Figure 57. Comparison of monthly net channel depletion estimates to values reported by Owen and Nance (1962).

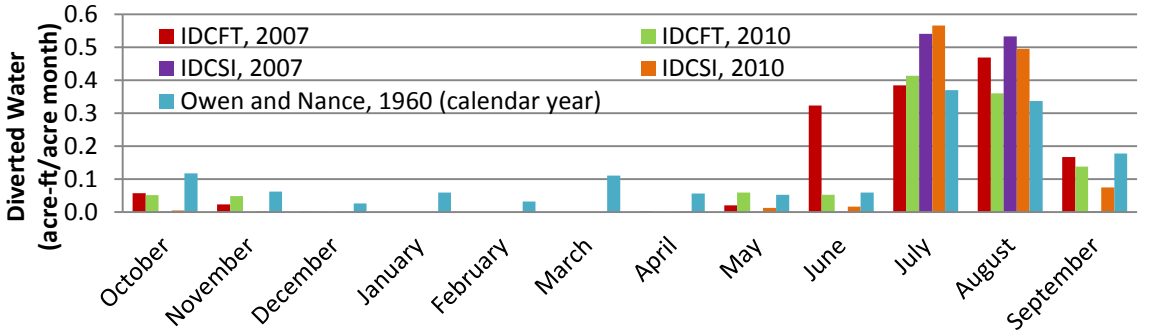

Figure 58. Comparison of monthly diversion estimates to values reported by Owen and Nance (1962).

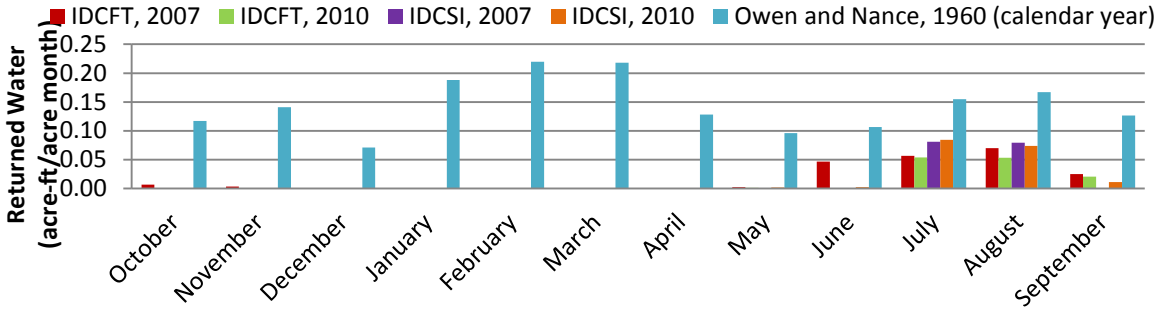

Figure 59. Comparison of monthly return estimates to values reported by Owen and Nance (1962).

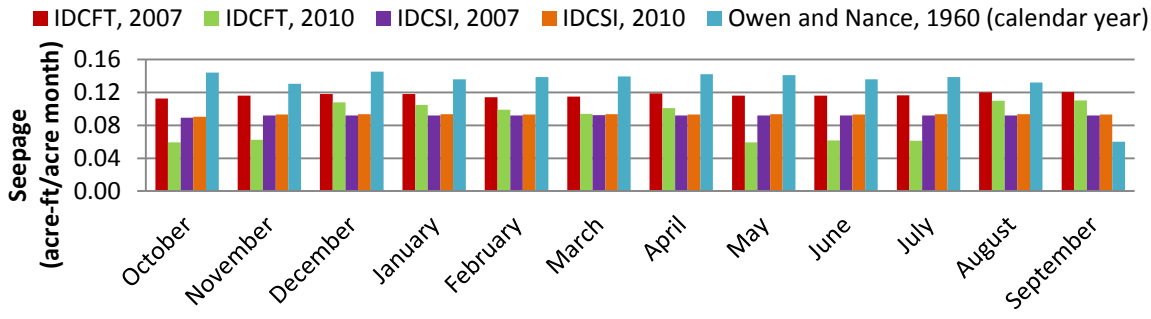

Figure 60. Comparison of monthly seepage estimates to values reported by Owen and Nance (1962).

4.3 Delta Water Quality Correlation

High levels of harmful water quality constituents have been observed in retuned agricultural runoff from Delta islands to in-Delta channels, suggesting that in-Delta water quality can be affected by agricultural returns. However, obtained water quality data are insufficient to determine the scale of these affects.

The developed DICU model estimates volumes of water diverted and returned on a higher resolution than existing DICU models and bases diversion and return locations on geography rather than simple geographical approximation, allocating diversion and return watersheds to each respective location. Land-use statistics for given watersheds can be determined through GIS analysis permitting correlations between agricultural land-use type and return water quality to be applied to locations. Additionally, the developed DICU model captures daily variations in diverted and returned water that are missed in monthly DICU models (Figures 61 and 62). For these reasons, if correlations between crop type and return water quality or estimates of return water quality can be made, the developed DICU model is expected to improve water quality estimates within the Delta.

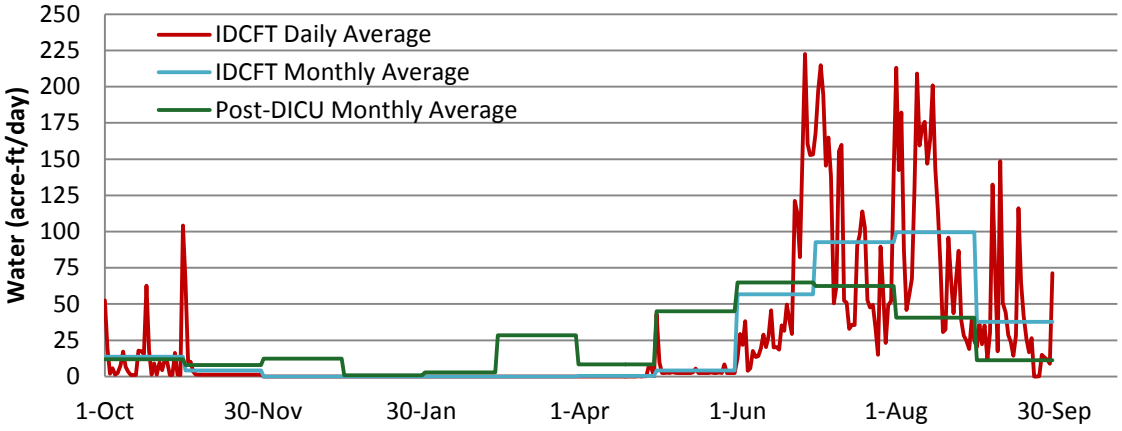

Figure 61. Comparison of Fabian Tract 2007 average daily vs. monthly diversion rates.

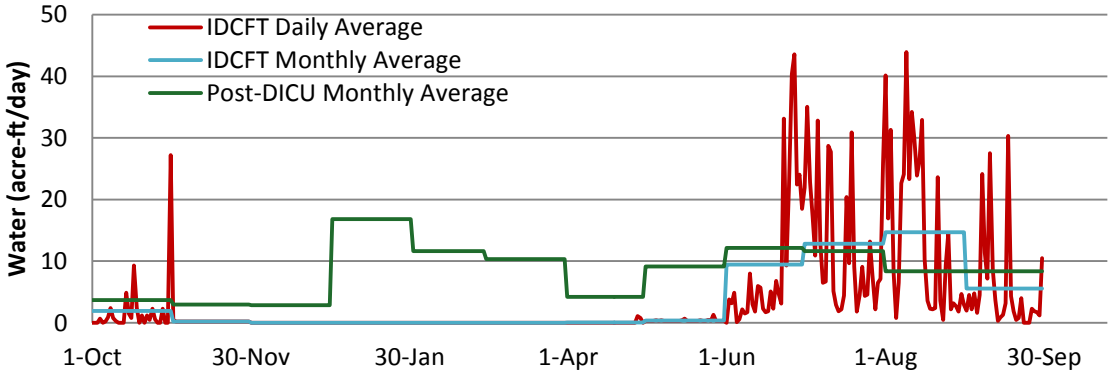

Figure 62. Comparison of Fabian Tract 2007 average daily vs. monthly return rates.

5 Time Estimate for Entire Delta Analysis

Based on the time requirements to analyze Fabian Tract and Staten Island using the methods described herein, assuming efficiency increases with practice and data acquisition can be applied to the entire Delta, time estimates to analyze the entire Delta were made (Table 3). A single person can likely model the entire Delta in approximately 27 months using the techniques described herein. However, if a team of three people were set to the task of modeling the entire Delta, they could likely accomplish the task in about 9 months.

Table 3. Time estimates to analyze the entire delta using the physically based modeling methods described herein.

Task	Rough Time Estimate	
	Person Weeks	Person Months
1. Identify Diversion and Return Locations using LIDAR and GIS	40	10
2. Ground-Truth Diversion and Return Locations	8	2
3. Model Integration	60	15
Total	110	27

6 Conclusions

In an on-going effort to better understand and manage the Delta, a collaborative, integrated approach was used to predict DICU and water quality on a higher resolution and base diversion and return locations on topography rather than simple geographical approximation. Fabian Tract and Staten Island were selected for this study.

Diversion and return location data and LIDAR DEM data were used to predict diversion and return locations on the Delta islands in a non-invasive manner. Diversion locations were listed in historical diversion and return data and water rights documentation, however some diversion locations and most return locations were not listed in the data and locations varied between data sets. Through GIS analysis accurate predictions of diversion and return locations were made. Most identified diversion and return locations were found to be valid through ground-truthing. Due to the close proximity of incorrectly documented diversion and return locations to existing locations, errors in diversion and return locations are not expected to have significant impacts on in-Delta diversion and return patterns but would result in local errors seen in field measurements. The non-invasive method used to determine diversion and return locations appears to be applicable throughout the Delta.

Significant differences exist between the ground-truthed diversion and return locations and those listed in the Sacramento-San Joaquin Delta Atlas (1995) as well as current DICU model. The quantity and trends of diversion and return locations ground-truthed on the islands of this study vary significantly from those of the Sacramento-San Joaquin

Delta Water Atlas. The Sacramento-San Joaquin Delta Atlas is not suggested for use in determining diversion and return locations within the Delta. Updates to the diversion and return locations in the Delta Water Atlas should be made. The quantity of diversion and return locations observed ground-truthing vary significantly from those listed in the current DICU model as well; however the trend of diversion and return locations on Fabian Tract and Staten Island in the current DICU model is similar to the observed trend during ground-truthing. Errors in the number of diversion and return locations in the current DICU model are not expected to significantly affect diversion and return patterns.

IDC was selected to calculate diversion and return rates from agricultural land-use. When compared to historical DICU data and other models, IDC-FT and IDC-SI net channel depletions and diversion estimates appeared valid. However, IDC-FT and IDC-SI return and seepage estimates varied from other existing models and historical data. The seepage rate assumed for the IDC model is an obvious weakness. The seepage rate used is based on a historical study of a single island. The soil and topology of the islands vary from island to island, as a result their seepage rates are also expected to vary. Additionally, studies have suggested model sensitivity to precipitation data. The use of different precipitation datasets as well as return flow fractions may have also contributed to the observed differences in seepage and return flow estimates. The trends of return flow in the IDC models do not match the post-DICU trends well. Through GIS analysis, the current DICU model allocation of agricultural runoff is expected to be incorrect. Updates to the diversion and return calculations and the allocation of returned water in the current DICU model should be made.

Water quality data were collected from various water quality monitoring studies in California and compared with estimated diversion and return data. High levels of harmful water quality constituents were observed in retuned agricultural runoff Delta islands to in-Delta streams and channels suggesting that in-Delta water quality can be affected by agricultural returns. However, current water quality data are insufficient to determine the scale of these affects. The model results from this study provide estimates of the volume of water diverted and returned from actual diversion and return locations on a daily time step, providing insight into daily agricultural diversion and return operations within the Delta that are missed in DICU models. As better correlations between crop type and return water quality are developed or estimates of return water quality are made, the a physically based model of DICU is expected to improve daily in-Delta water quality estimates.

Leaching practices are not accounted for in the physically based model of DICU described herein. However, the developed model permits the addition of scheduled irrigation practices. Leaching practices are expected to significantly impact the volume of water diverted and returned from Delta Islands as well as the water quality of in-Delta streams and channels. Once known, in-Delta leaching practices should be accounted for.

To improve DICU and water quality estimates in the Delta, further actions are required. These actions include:

1. Data acquisition of in-Delta agricultural practices
    a. Crop irrigation techniques
    b. Fertilizer and pesticide application processes
    c. Soil leaching schedules and processes
    d. Seepage analysis
2. In-Delta water quality sampling/testing
    a. Analysis of return water quality from various crops throughout the irrigation season
    b. Analysis of channel water quality throughout the irrigation season, noting periods when agricultural runoff is being returned to Delta streams and channels

References

Allen, R.G., Pereira, L.S., Raes D., and Smith M. (1998). "Crop Evapotranspiration: Guidelines for Computing Crop Water Requirements," FAO Irrigation and Drainage, No. 56, P.290.

Beaulac, M.N., and Reckhow, K.H. (1982). "An examination of land use-Nutrient export relationships," *Water Resources Bulletin*, 18, pp.1013-1022.

Bedient, P.B., Huber, W.C., and Vieux B.E. (2008). Hydrology and Floodplain Analysis Fourth Edition, Prentice-Hall, Inc, Upper Saddle River, NJ.

California Department of Fish and Game (DFG) (1991). *Fish Screen and Fish Passage Project*, Salmon, Steelhead Trout and Anadromous Fishes Restoration and Enhancement Program.

California Department of Water Resources (DWR) (1995). *Sacramento-San Joaquin Delta Atlas*, State of California Department of Water Resources, Sacramento, CA.

California Department of Water Resources (DWR) (1998, 1999, 2000, 2001). Annual Land & Water Use Estimates, Irrigated Crop Acres and Water Use. Accessed online (5 March 2012):
http://www.water.ca.gov/landwateruse/anaglwu.cfm

California Department of Water Resources (2007). *Lidar data for the Delta Area of California*, California Department of Water Resources Delta-Suisun Marsh Office Division of Flood Management.

California Department of Water Resources (2011). IWFM: Integrated Water Flow Model-Demand Calculator (IDC). Accessed online (14 November 2011):
http://baydeltaoffice.water.ca.gov/modeling/hydrology/IWFM/IDC/index_IDC.cfm

Central Valley Regional Data Center (CV RDC). "CV RDC Data Request." Compiled on 11/3/2011 for Lucas Siegfried and Dr. William Fleenor.

Courault, D., Bernard, S., and Olioso, O. (2005). Review on estimation evapotranspiration from remote sensing data: From empirical to numerical modeling approaches, Irrigation and Drainage Systems, 19, P.223-249.

Crago, R.D. (2000). “Conservation and variability of the evaporative fracture during the daytime,” *Journal of Hydrology*, 180, 1-4, P.173-194.

Deverel, S.J., Ingrum, T., Hart, C., and Drexler, J. (2012). *Simulation of Vertical Marsh Accretion in the Sacramento-San Joaquin Delta, California, USA*. Report created in combination with HydroFocus, Inc. and US Geological Survey California Water Science Center.

Dogrul, E.C. Kadir, T. N. and Chung, F. I. (2011). “Root Zone Moisture Routing and Water Demand Calculations in the Context of Integrated Hydrology,” *Journal of Irrigation and Drainage Engineering*, Vol. 137, No. 6, P. 359-366.

Dogrul, E.C., Schmid, W., Hanson, R.T., Kadir, T., and Chung F. (2011). *Integrated Water Flow Model and Modfllow-Farm Process: A Comparison of Theory, Approaches, and Futures of Two Integrated Hydrologic Models*, California Department of Water Resources, Integrated Hydrological Models Development Unit, Modeling Support Branch, Bay-Delta Office, Sacramento CA.

Evett S.R. (2000). “Water and energy balances of soil-plant-atmosphere interfaces,” Hand Book of Soil Science, M.E. Sumner Ed., CRC Press: Boca Raton; A129-A182.

Hoffman, G.J. (2010). *Salt Tolerance of Crops in the Southern Sacramento-San Joaquin Delta*, California Environmental Protection Agency, State Water Resources Control Board, Division of Water Rights, CA.

HydroFocus, Inc. (2012). *What is the Fugure of Farming on Organic Soils in the Sacramento-San Joaquin Delta?*, draft report prepared for Metropolitan Water District of Southern California.

Integrated Hydrological Models Development Unit (IHMD) (2011). *Integrated Water Flow Model IWFM v3.02 revision 36 Theoretical Documentation (IWFM Theoretical Documentation)*, Modeling Support Branch, Bay-Delta Office.

Integrated Hydrological Models Development Unit (IHMD) (2011a). *IWFM Demand Calculator: IDC v4.0 Theoretical Documentation and User’s Manual*, Modeling Support Branch, Bay-Delta Office.

Jackson, R.D., Reginato, R.J. and Idso, S.B. 1977. “Wheat canopy temperature: A practical tool for evaluating water requirements,” Water Resources Research, 13, PP. 651-656.

Jordan, T.E., Correll, D.L., and Weller, D.E. (1997). ”Effects of Agriculture on Discharges of Nutrients from Coastal Plain Watersheds of Chesapeake Bay,” *Journal of Environmental Quality*, 26, pp.836-848.

Kadir, T. 2006. “Chapter 7: Estimates for Consumptive Water Demands in the Delta using DETAW,” *Methodology for Flow and Salinity Estimates in the Sacramento-San Joaquin Delta and Suisun Marsh*, 27th Annual Progress Report.

Kadir, T. “DETAW 2007.” Email to Lucas Siegfried. May 2, 2012.

Lenat, D.R. and Crawford, J.K. (1994). “Effects of land use on water quality and aquatic biota of three North Carolina Piedmont streams,” Hydrobiologia, 294, pp.185-199.

Liang, L. “DICU Fabian Tract Model Area.” Email to Lucas Siegfried. August 6, 2012.

Lund, J., Hanak, E., Fleenor, W., Bennett, W., Howitt, R., Mount, J., and Moyle, P. (2010). *Comparing Futures for the Sacramento-San Joaquin Delta*, University of California Press, Berkeley, CA.

Lund, J., Hanak, E., Fleenor, W., Howitt, R., Mount J., and Moyle, P. (2007). *Envisioning Futures for the Sacramento-San Joaquin Delta*, Public Policy Institute of California, San Francisco, CA.

Madani, K., and Lund, J. (2011). C*alifornia’s Sacramento-San Joaquin Delta Conflict: from Cooperation to Chicken*, Water Science and Policy Center, Department of Environmental Sciences, Riverside, CA and Department of Civil and Environmental Engineering, University of California, Davis, CA.

Marvin Jung and Associates, Inc. (2000). *Revision of Representative Delta Island Return Flow Quality for DSM2 and DICU Model Runs*, Municipal Water Quality Investigations Program, DWR DPLA, Sacramento, CA.

Medellin-Azuara, J. (2012). Average crop ET water demands in the Sacramento-San Joaquin Delta attained through verbal communication and email, UC Davis Center for Watershed Sciences, Davis, CA. Attained February, 23, 2012.

Norman, J.M., and Becker, F. (1995). Terminology in infrared remote sensing of natural surfaces,Remote Sensing Reviews, 12, P.159–173.

Owen and Nance (1962). *Hydrology of the Sacramento-San Joaquin Delta*, Paper presented at ASCE Hydraulics Division Conference, Davis, CA.

Resource Management Associates (RMA) (2005). *Flooded Islands Pre-Feasibility Study*, RMA Delta Model Calibration Report prepared for California Department of Water Resources, California Bay-Delta Authority.

Rojstaczer, S.A., and Deverel, S.J. (1993). *Time dependence of atmospheric carbon inputs from drainage of organic soils: Geophysical Research Letters*, v. 20, p. 1,383–1,386.

Rojstaczer, S.A., Hamon, R.E., Deverel, S.J., and Massey, C.A. (1991). *Evaluation of selected data to assess the causes of subsidence in the Sacramento- San Joaquin Delta*, California: U.S. Geological Survey Open-File Report 91-193, p.16.

Sclanlon, B., Keese, K., Bonal, N., Deeds, N., Kelley, V., and Litvak, M. (2005). Evapotranspiration Estimates with Emphasis on Groundwater Evapotranspiration in Texas, Report prepared for the Texas Water Development Board.

SEBAL North America (2012). “SEBAL.” Accessed online (30 September 2012): <http://www.sebal.us/>

State of California Department of Water Resources Division of Planning (1995). *Estimation of Delta Island Diversion and Return Flows*. California Department of Water Resources, Sacramento, CA.

Soil Survey Staff, Natural Resources Conservation Service, United States Department of Agriculture.
Soil Survey Geographic (SSURGO) Database for [Survey Area, State]. Accessed online (10 Sept. 2011):
<http://soildatamart.nrcs.usda.gov>

State of California (2007).“About CALFED.” CALFED Bay Delta Program. Accessed online (15 Aug. 2011): <http://calwater.ca.gov/calfed/about/index.html>

State of California Department of Water Resources Division of Planning (DWR) (1991). *Trihalomethane Formation Potential in the Sacramento-San Joaquin Delta Mathematical Model Development*. California Department of Water Resources, Sacramento, CA

Templin, W.E. and Cherry, D.E. (1997). “Drainage-Return, Surface-Water Withdawal, and Land-Use Data for the Sacramento-San Joaquin Delta, with Emphasis on Twitchell Island, California,” U.S. Geological Survey, 97-350, p. 6217-34.

Thompson, J. (1957). *Settlement Geography of the Sacramento-San Joaquin Delta*, California, dissertation, Stanford University.

Thornthwaite, C.W. (1984). “An Approach Toward a Rational Classification of Climate,” Geography Review, 38, pp.55-94.

Tilman, D. Cassman, K.G., Matson, P.A., Naylor, R., and Polasky, S. (2002). “Agricultural sustainability and intensive production practices,” *Nature*, 418, pp.671-677.

Tracy Weather Station Data from the California Irrigation Management Information System (CIMIS), Department of Water Resources. Web. 5 January 2012. <http://wwwcimis.water.ca.gov>

United States Department of Agriculture (USDA), National Agricultural Statistics Service, *2010 California Cropland Data Layer*. Web. 20 Sept. 2011. <http://www.nass.usda.gov/research/Cropland/metadata/metadata_ca10.htm>

USDA, Soil Conservation Service. 1985. *National engineering handbook*. Washington (DC): US Department of Agriculture. Section 4, Hydrology, Chapters 9 and 10.

U.S. Geological Survey (USGS) (2000). “Delta Subsidence in California,” *The sinking heart of the State.* US Department of the Interior, US Geological Survey, FS-005-00.

USGS (2011). "Summary of MODFLOW-2005." Accessed online (6 Jan. 2012): <http://water.usgs.gov/nrp/gwsoftware/modflow2005/modflow2005.html>.

Van Genuchten, M. Th., and Hoffman, G. J. (1984). “8.1 Analysis of Crop Salt Tolerance Data,” in Shainberg, I. and Shalhevet, J. “Soil Salinity under Irrigation, Processes and Management,” *Ecological Studies*, 51, pp. 258-271.

Whipple AA, Grossinger RM, Rankin D, Stanford B, Askevold RA. 2012. Sacramento-San Joaquin Delta Historical Ecology Investigation: Exploring Pattern and Process. Prepared for the California Department of Fish and Game and Ecosystem Restoration Program. A Report of SFEI-ASC’s Historical Ecology Program, Publication #672, San Francisco Estuary Institute-Aquatic Science Center, Richmond, CA.

Appendix

Appendix A: DICU on Twitchell Island from December 1959 to December 1960 (Owen and Nance 1962)

DISTRIBUTION OF SEEPAGE INFLOW TO TWITCHELL ISLAND FOR STUDY PERIOD

Month	Percent
December 1959	5.97
January 1960	8.57
February 1960	7.75
March 1960	8.63
April 1960	8.07
May 1960	8.24
June 1960	8.26
July 1960	8.44
August 1960	8.37
September 1960	8.07
October 1960	8.24
November 1960	7.82
December 1960	3.57

SUMMARY OF MEASURED AND COMPUTED HYDROLOGIC DATA (Acre-feet)

Month	Item			
	SI	P	CU	PO
December 1959	26	258	138	29
January 1960	215	1,011	166	68
February 1960	115	787	180	79
March 1960	401	551	269	79
April 1960	203	321	857	46
May 1960	190	97	1,208	34
June 1960	215	0	1,214	38
July 1960	1,341	0	1,519	56
August 1960	1,221	0	1,520	60
September 1960	643	0	1,059	46
October 1960	425	18	470	42
November 1960	225	1,253	285	51
December 1960	95	59	93	25
Total	5,315	4.355	8,978	6,59

CHANGE IN SOIL MOISTURE

Date of Measurement	Change in soil moisture between measurements: inches	Cumulative change in soil moisture: inches	acre-fe
December 10, 1959			
	+ 2.03	+ 2.03	+ 55
January 19, 1960			
	+ 2.52	+ 4.55	+123
February 22, 1960			
	- 5.14	- 0.59	- 16
June 7, 1960			
	- 0.50	- 1.09	- 29
July 13, 1960			
	- 0.92	- 2.01	- 54
August 23, 1960			
	- 1.35	- 3.36	- 91
October 12, 1960			
	+ 4.16	+ 0.80	+ 21
December 14, 1960			

COMPUTED MONTHLY CHANGES IN SOIL MOISTURE (acre-feet)

Month	ΔSM	Cumulative ΔSM
December 1959	215	215
January 1960	902	1,117
February 1960	398	1,515
March 1960	419	1,934
April 1960	-304	1,630
May 1960	-766	864
June 1960	-880	- 16
July 1960	-223	-239
August 1960	-393	-632
September 1960	-382	-1,014
October 1960	52	-962
November 1960	1,160	+198
December 1960	20	+218

SEEPAGE (Acre-feet per month)

December 1959	366
January 1960	524
February 1960	474
March 1960	528
April 1960	494
May 1960	504
June 1960	506
July 1960	517
August 1960	512
September 1960	494
October 1960	504
November 1960	479
December 1960	218

INDICATED ADJUSTMENTS TO COMPUTED OUTFLOW CONSIDERING CHANGE IN SOIL MOISTURE

Month	CFS	% of Computed Outflow
December 1959	-500	-6.2
January 1960	-1500	-12.7
February 1960	-700	-1.9
March 1960	-700	-2.2
April 1960	+500	+3.1
May 1960	+1300	+11.2
June 1960	+1500	+38.9
July 1960	+400	+16.6
August 1960	+600	+26.7
September 1960	+600	+11.8
October 1960	-100	-1.9
November 1960	-2000	-17.5
December 1960	-700	-0.4

(Plus values indicate an increase in outflow)

Appendix B: NODCU method to calculate Delta Island diversions and drainages

(DWR 1995)

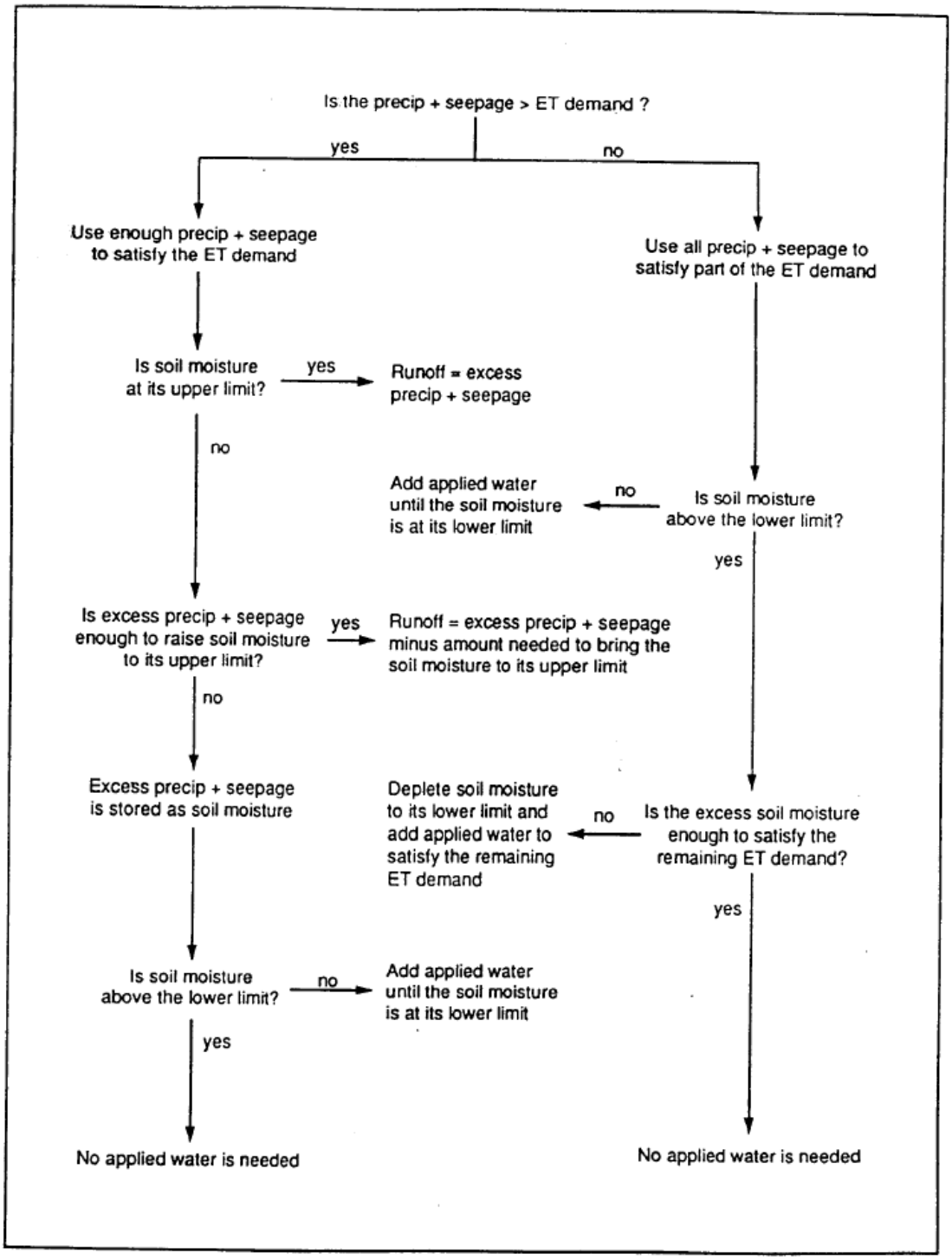

Appendix C: Deltal Island Return Flow Water Quality Regressions (Marvin Jung and Associates, Inc. 2000)

Table 4. TFPC, DOC, and UVA-254nm Regression Equations

DOC subarea	Equations *UVA in cm^{-1} and TFPC in µg/l and DOC in mg/L*	Data range n = 953	Correlation coefficients
All (Fig. 4a-b)	TFPC = 36.815+7.52*DOC	TFPC(8.86-917.2)	R = 0.86
	UVA = 1.2415 + 20.46*DOC	UVA(0.059-3.86)	R = 0.95
All (Fig. 5a-b)	TFPC = 37.535 + 164.46*UVA	DOC (2 – 98)	R = 0.87
	UVA = 0.02374 + 0.04415*DOC		R = 0.95

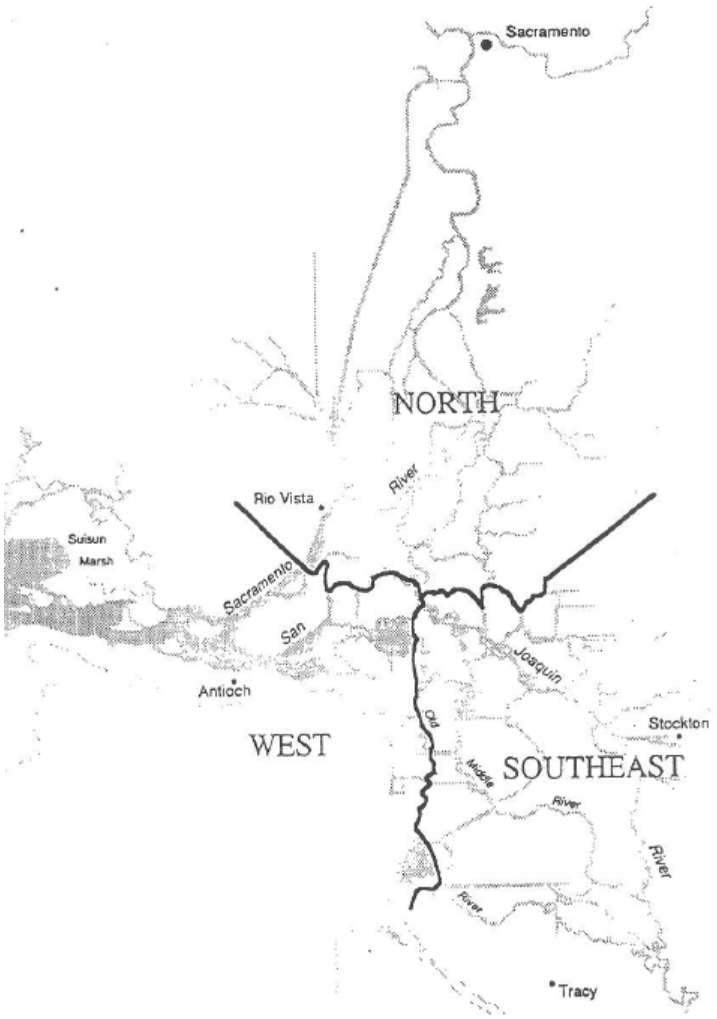

Figure 6. Bulletin 123 Delta Subregions

Table 6a. West Delta Drainage
Correlation Matrix Table

STAT. BASIC STATS	Correlations (drwg3.sta) Marked correlations are significant at p < .05000 N=168 (Casewise deletion of missing data)							
Variable	EC	TDS	BR	CA	CL	MG	NA	SO4
EC	1.00	1.00 *	.96 *	.73 *	.99 *	.95 *	.99 *	.92 *
TDS	1.00 *	1.00	.96 *	.75 *	.99 *	.96 *	.98 *	.94 *
BR	.96 *	.96 *	1.00	.58 *	.98 *	.87 *	.98 *	.82 *
CA	.73 *	.75 *	.58 *	1.00	.68 *	.86 *	.63 *	.85 *
CL	.99 *	.99 *	.98 *	.68 *	1.00	.92 *	.99 *	.88 *
MG	.95 *	.96 *	.87 *	.86 *	.92 *	1.00	.91 *	.95 *
NA	.99 *	.98 *	.98 *	.63 *	.99 *	.91 *	1.00	.88 *
SO4	.92 *	.94 *	.82 *	.85 *	.88 *	.95 *	.88 *	1.00

Table 6a Correlation Plots for West Delta Drainage

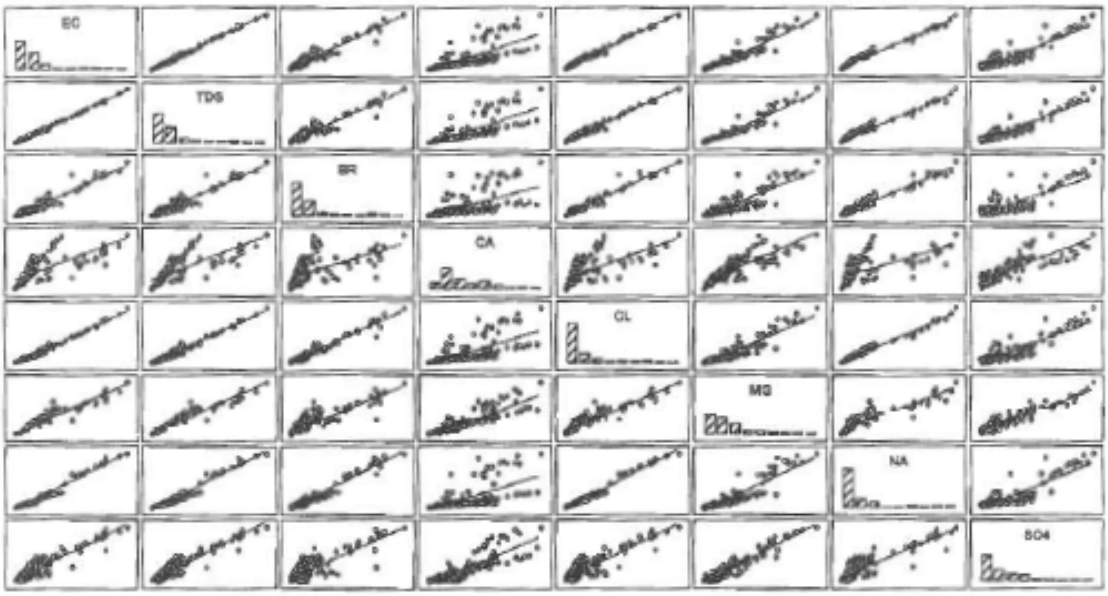

Table 6b. North Delta Drainage Correlation Matrix Table

STAT. BASIC STATS	Correlations (drwq3.sta) Marked correlations are significant at p < .05000 N=257 (Casewise deletion of missing data)							
Variable	EC	TDS	BR	CA	CL	MG	NA	SO4
EC	1.00	.98 *	.77 *	.92 *	.95 *	.91 *	.93 *	.85 *
TDS	.98 *	1.00	.72 *	.94 *	.91 *	.91 *	.90 *	.87 *
BR	.77 *	.72 *	1.00	.58 *	.85 *	.59 *	.81 *	.39 *
CA	.92 *	.94 *	.58 *	1.00	.79 *	.97 *	.74 *	.88 *
CL	.95 *	.91 *	.85 *	.79 *	1.00	.79 *	.95 *	.71 *
MG	.91 *	.91 *	.59 *	.97 *	.79 *	1.00	.71 *	.83 *
NA	.93 *	.90 *	.81 *	.74 *	.95 *	.71 *	1.00	.73 *
SO4	.85 *	.87 *	.39 *	.88 *	.71 *	.83 *	.73 *	1.00

Table 6b Correlation Plots for North Delta Drainage

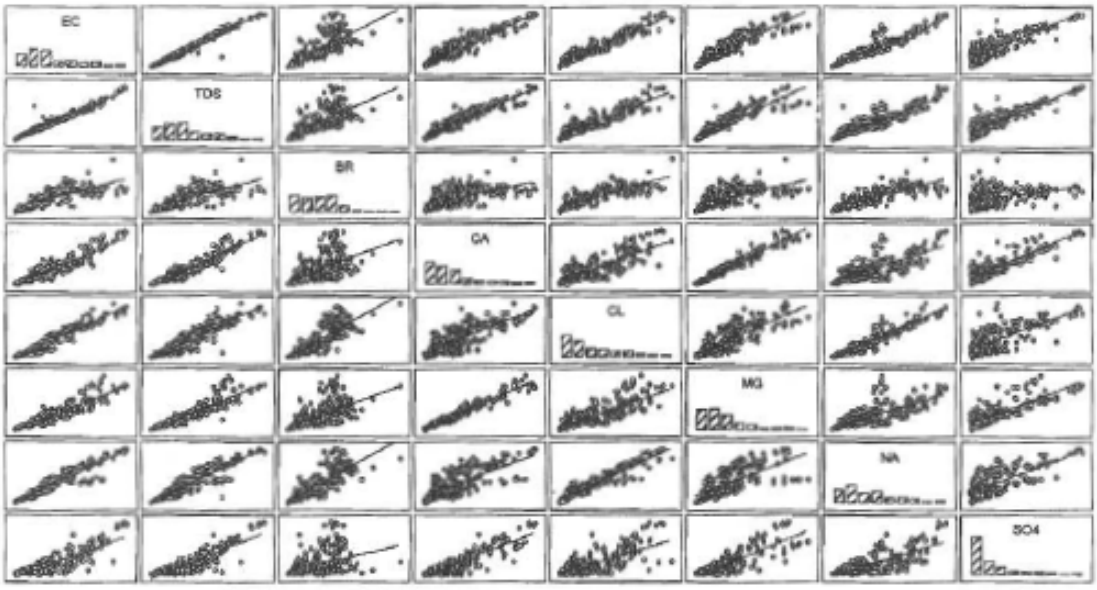

Table 6c. Southeastern Delta Drainage Correlation Matrix Table

STAT. BASIC STATS	Correlations (drwq3.sta) Marked correlations are significant at p < .05000 N=353 (Casewise deletion of missing data)							
Variable	EC	TDS	BR	CA	CL	MG	NA	SO4
EC	1.00	.98 *	.86 *	.95 *	.96 *	.97 *	.96 *	.80 *
TDS	.98 *	1.00	.82 *	.96 *	.92 *	.96 *	.93 *	.84 *
BR	.86 *	.82 *	1.00	.78 *	.93 *	.79 *	.84 *	.47 *
CA	.95 *	.96 *	.78 *	1.00	.88 *	.98 *	.84 *	.81 *
CL	.96 *	.92 *	.93 *	.88 *	1.00	.90 *	.93 *	.64 *
MG	.97 *	.96 *	.79 *	.98 *	.90 *	1.00	.89 *	.83 *
NA	.96 *	.93 *	.84 *	.84 *	.93 *	.89 *	1.00	.75 *
SO4	.80 *	.84 *	.47 *	.81 *	.64 *	.83 *	.75 *	1.00

Table 6c Correlation Plots for Southeast Delta Drainage

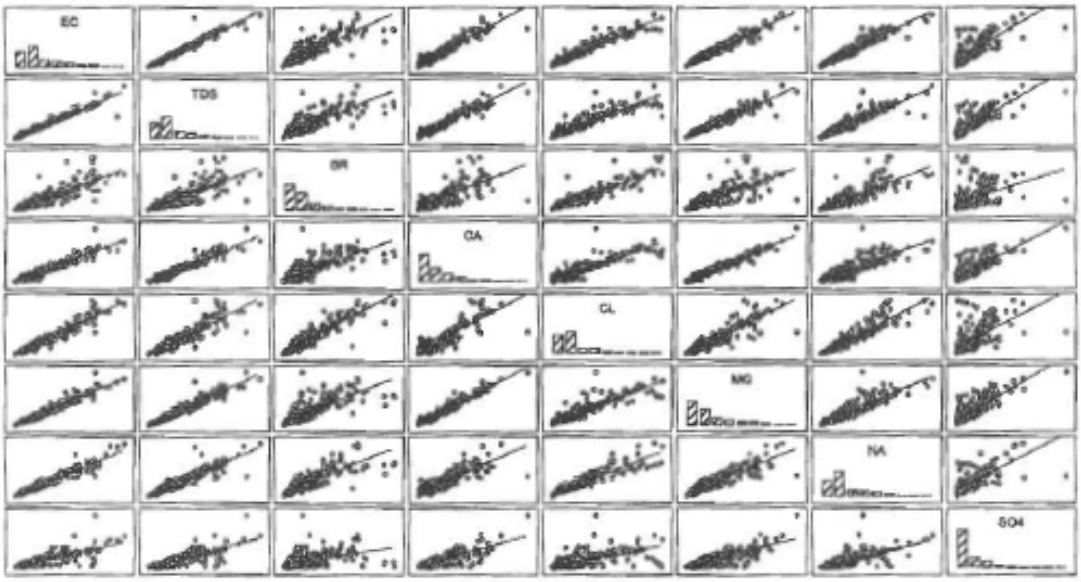

Appendix D: California Water Use, by Crop, 2003 (DWR 2012)

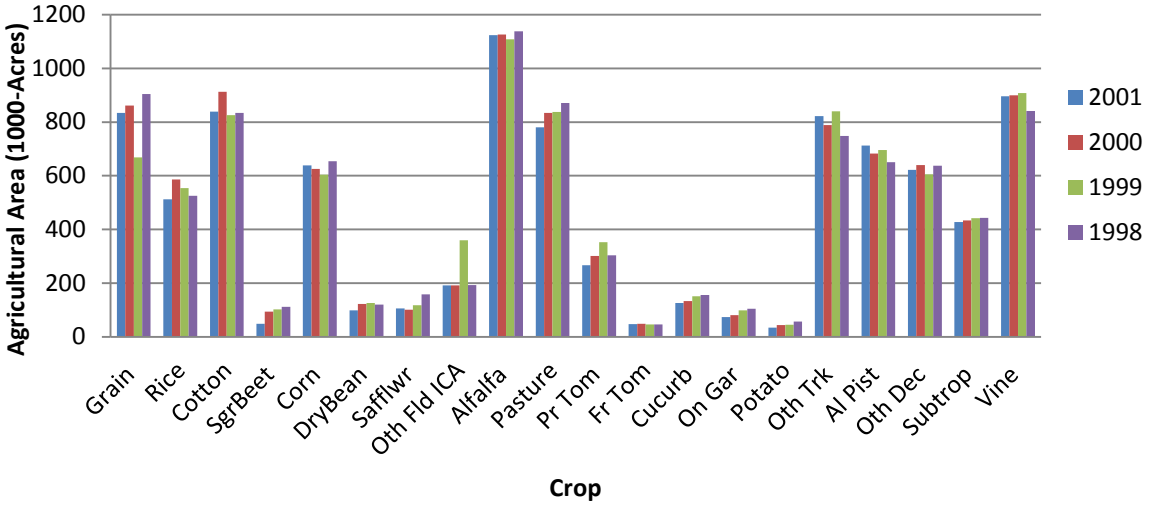

Figure 63. Agricultural land use in California.

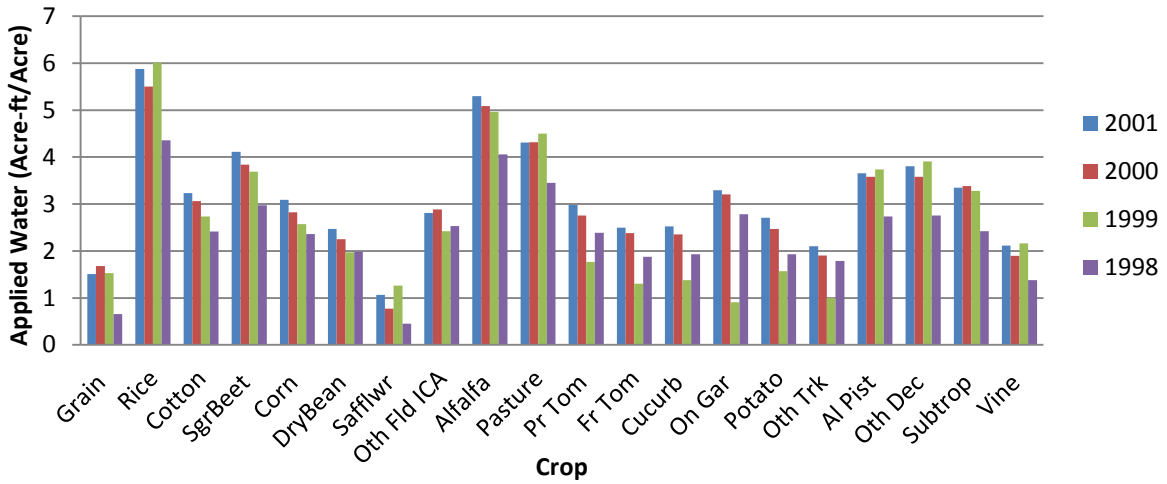

Figure 64. Applied water in California.

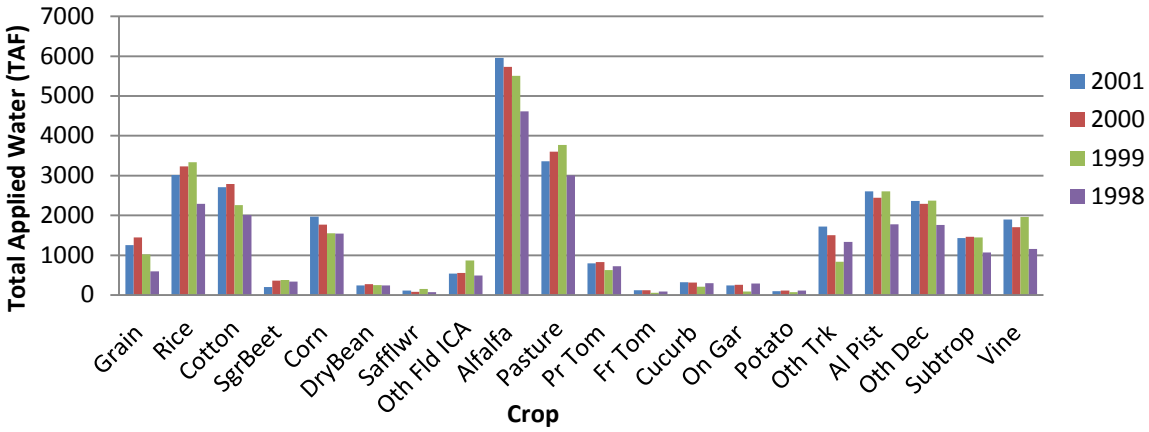

Figure 65. Total applied water in California.

Appendix E: IDC Model Run Results

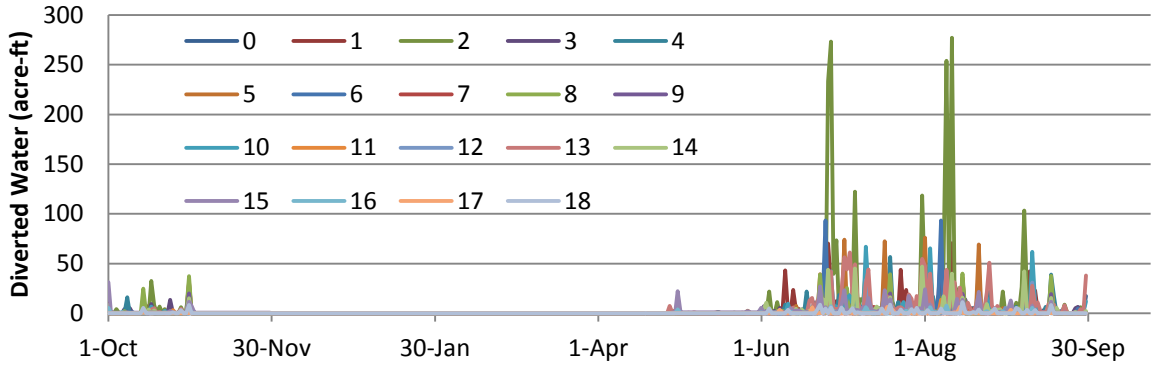

Figure 66. 2007, daily diverted water on Fabian Tract from ground-truthed diversion locations.

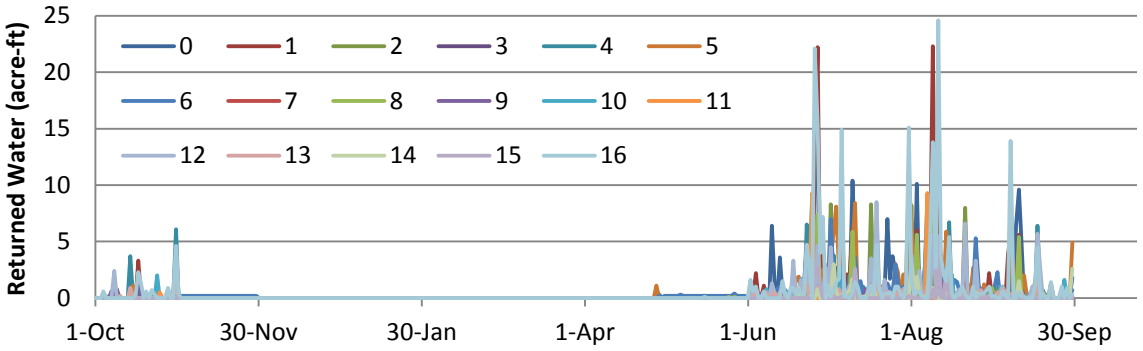

Figure 67. 2007, daily returned water on Fabian Tract from ground-truthed return locations.

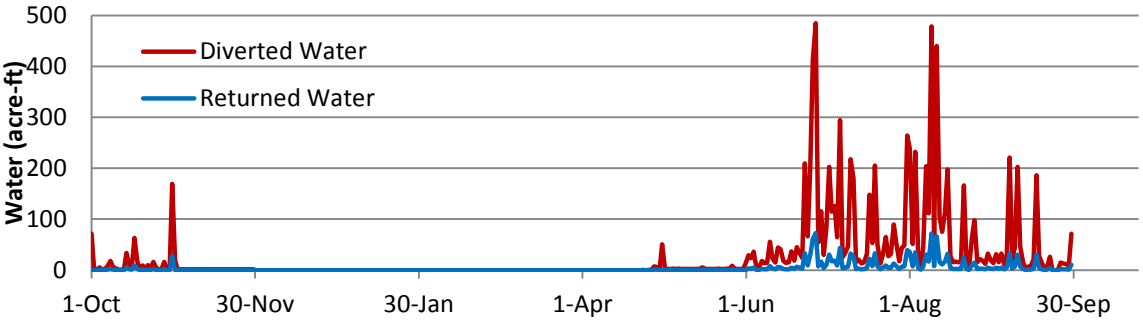

Figure 68. 2007, total daily diverted and returned water using a saturated hydraulic conductivity of 0.05 µm/s for all ponded elements and assuming a constant seepage rate onto Fabian Tract of 0.025 inches per foot rooting depth per month.

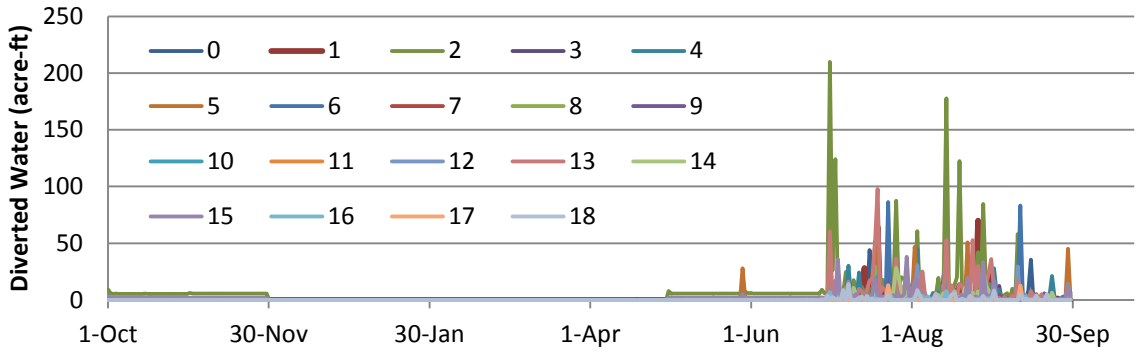

Figure 69. 2010, daily diverted water on Fabian Tract from ground-truthed diversion locations.

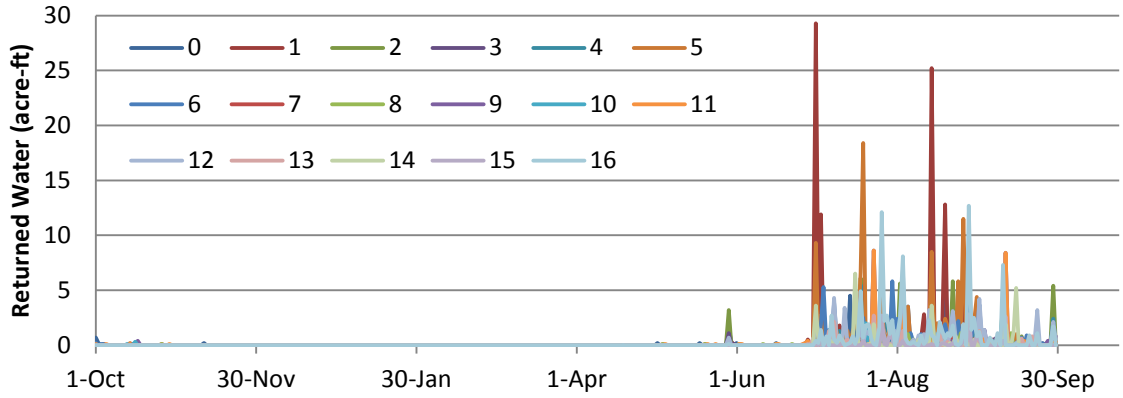

Figure 70. 2010, daily returned water on Fabian Tract from ground-truthed return locations.

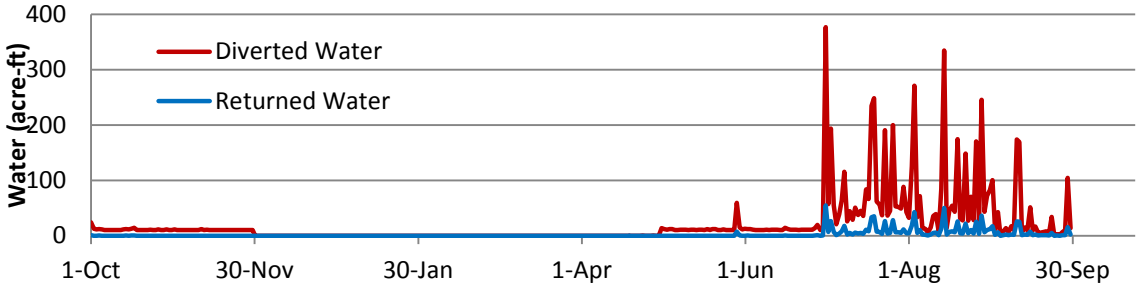

Figure 71. 2010, total daily diverted and returned water using a saturated hydraulic conductivity of 0.05 µm/s for all ponded elements and assuming a constant seepage rate onto Fabian Tract of 0.025 inches per foot rooting depth per month.

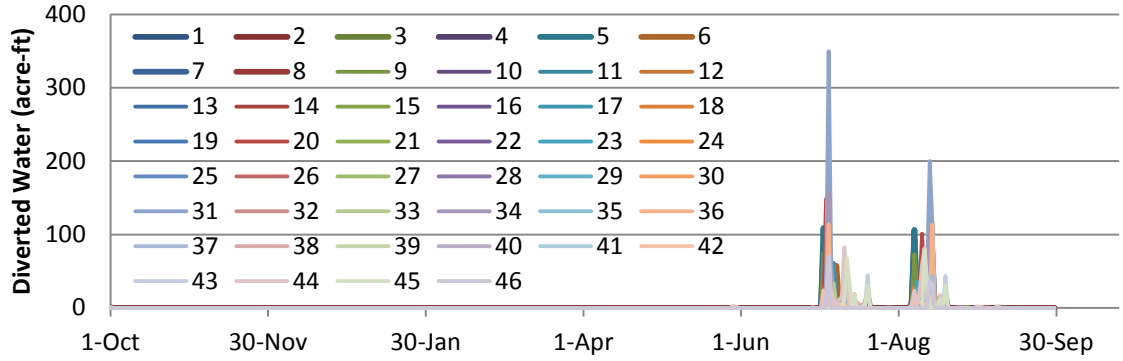

Figure 72. 2007, daily diverted water on Staten Island from ground-truthed diversion locations.

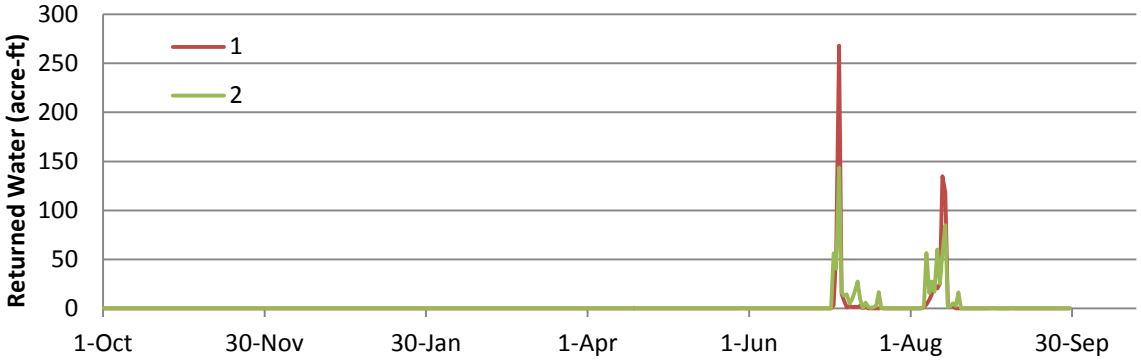

Figure 73. 2007, daily returned water on Staten Island from ground-truthed return locations.

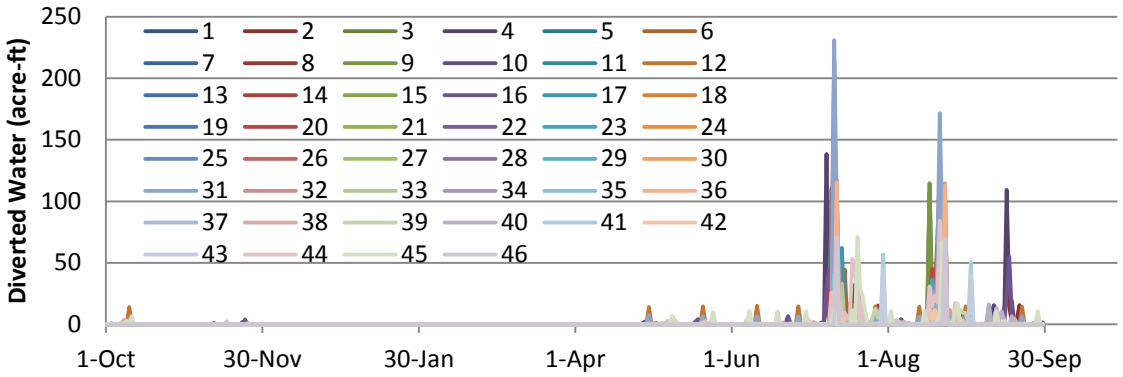

Figure 74. 2010, daily diverted water on Staten Island from ground-truthed diversion locations.

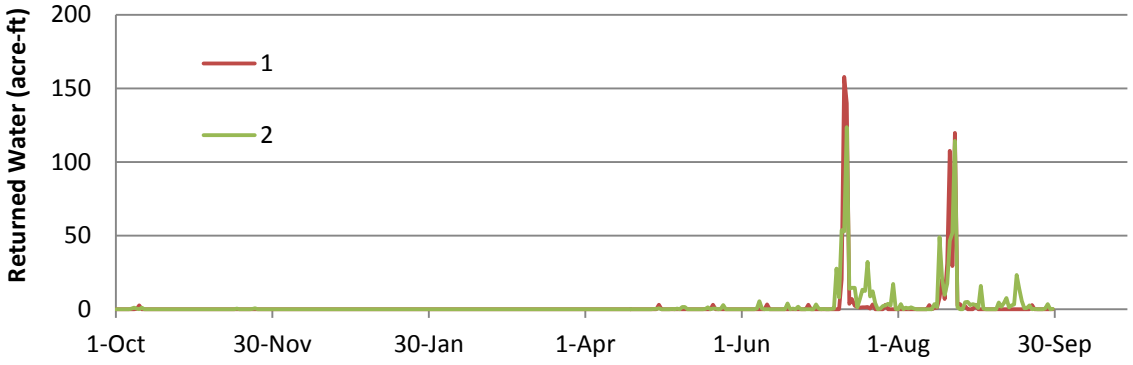

Figure 75. 2010, daily returned water on Staten Island from ground-truthed return locations.

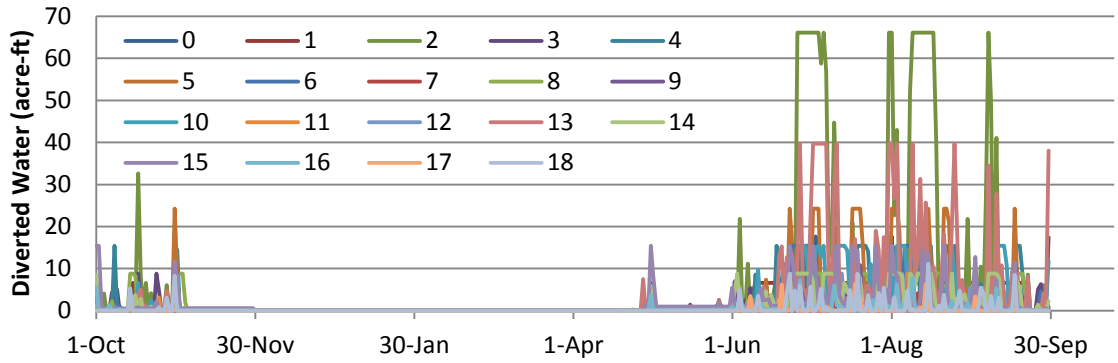

Figure 76. 2007, daily diverted water on Fabian Tract from ground-truthed diversion locations with limits applied to the diversion rate.

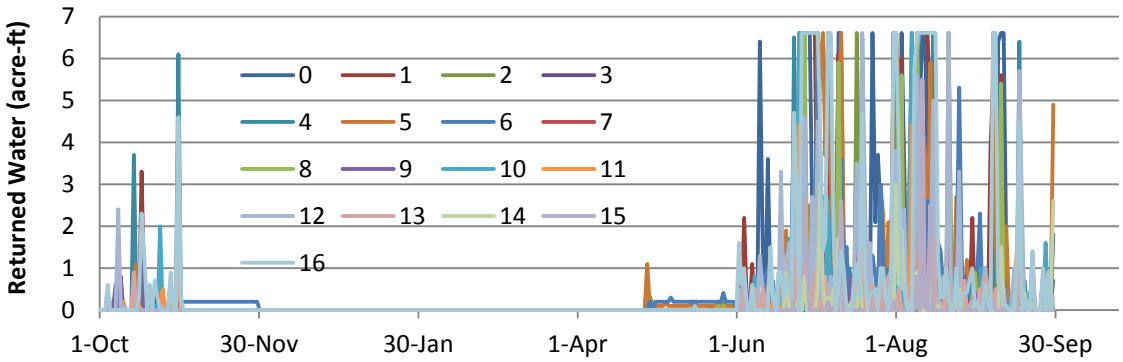

Figure 77. 2007, daily returned water on Fabian Tract from ground-truthed return locations with limits applied to the return rate.

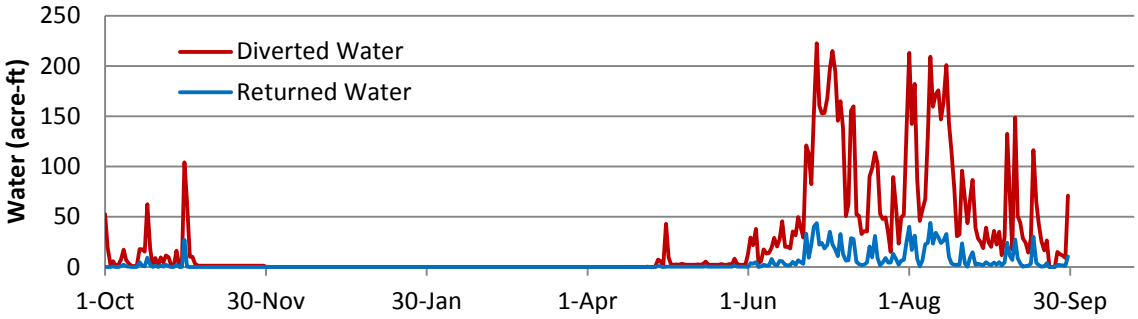

Figure 78. 2007, total daily diverted and returned water using a saturated hydraulic conductivity of 0.05 µm/s for all ponded elements, assuming a constant seepage rate onto Fabian Tract of 0.025 inches per foot rooting depth per month, and applying diversion and return rate limits.

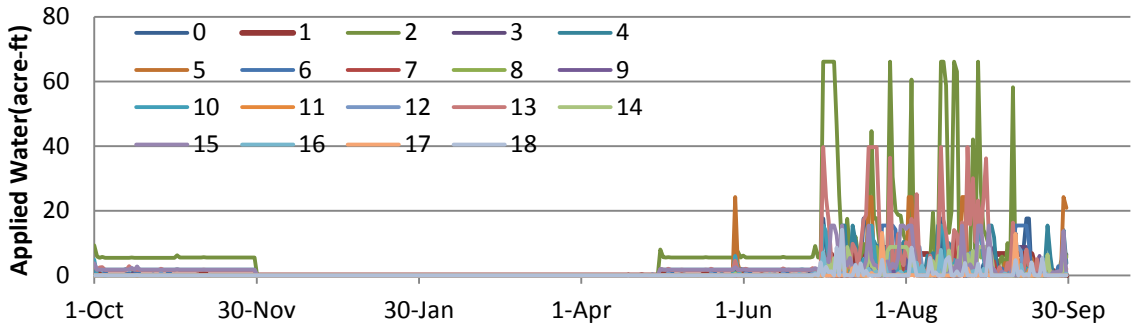

Figure 79. 2010, daily diverted water on Fabian Tract from ground-truthed diversion locations with limits applied to the diversion rate.

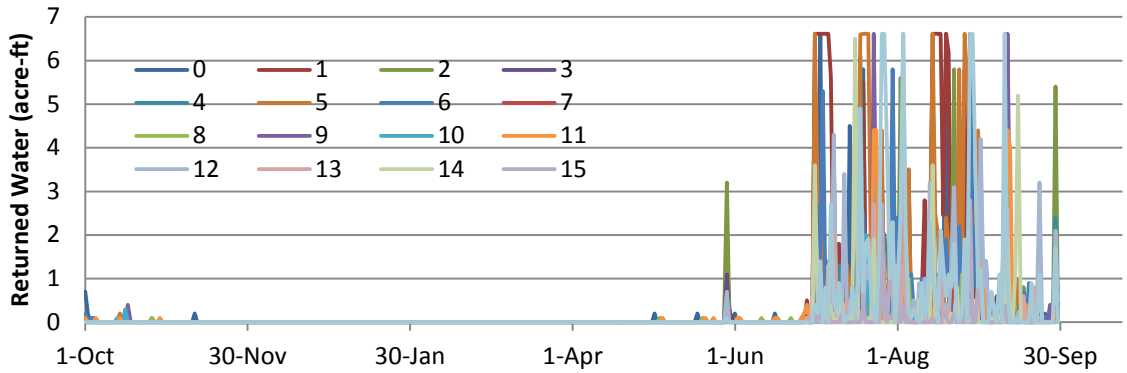

Figure 80. 2010, daily returned water on Fabian Tract from ground-truthed return locations with limits applied to the return rate.

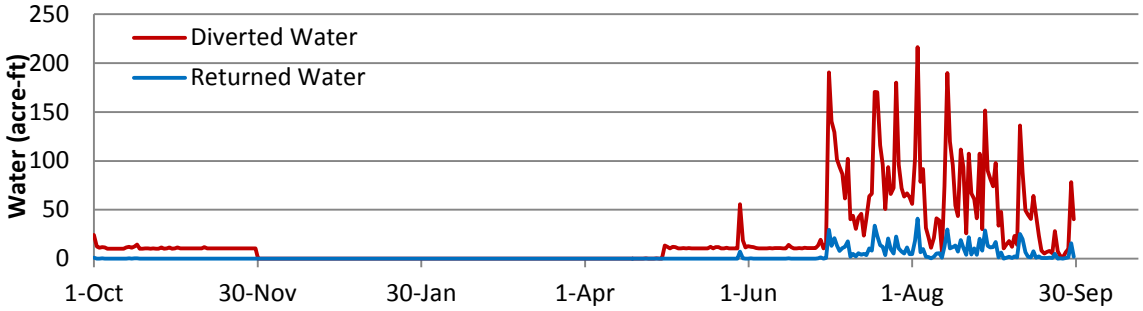

Figure 81. 2010, total daily diverted and returned water using a saturated hydraulic conductivity of 0.05 µm/s for all ponded elements, assuming a constant seepage rate onto Fabian Tract of 0.025 inches per foot rooting depth per month, and applying diversion and return rate limits

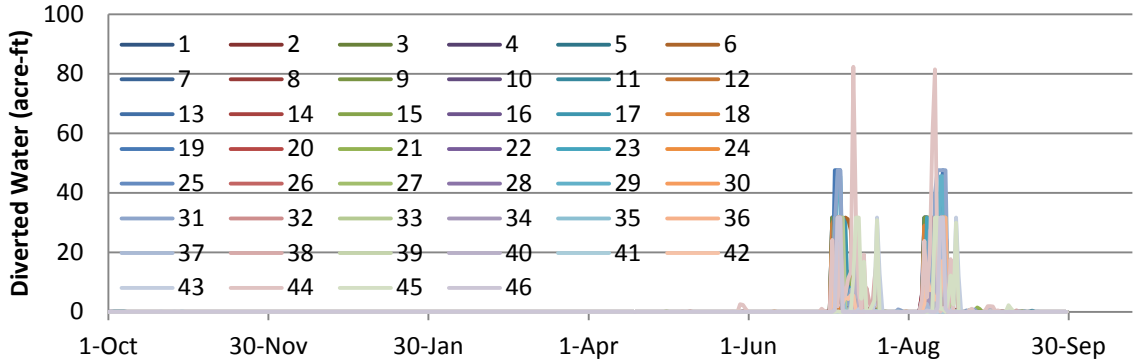

Figure 82. 2007, daily diverted water on Staten Island from ground-truthed diversion locations with limits applied to the diversion rate.

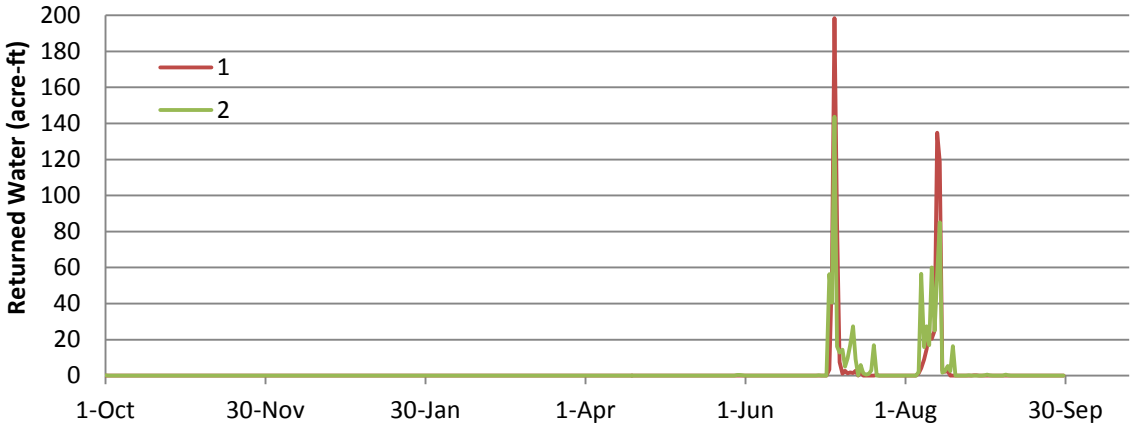

Figure 83. 2007, daily returned water on Staten Island from ground-truthed return locations with limits applied to the return rate.

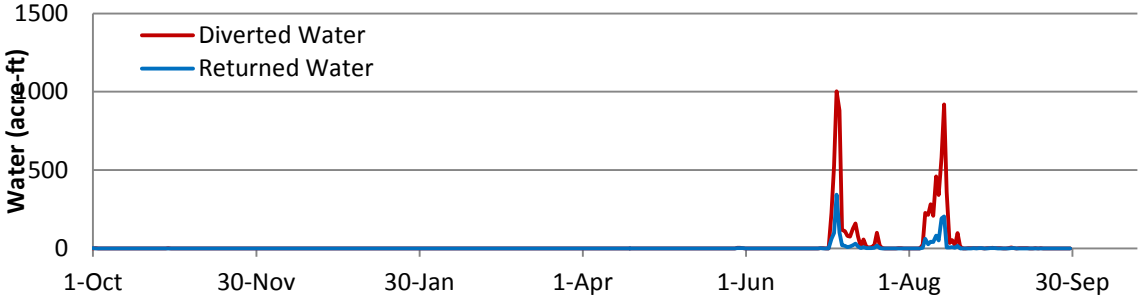

Figure 84. 2007, total daily diverted and returned water using a saturated hydraulic conductivity of 0.05 µm/s for all ponded elements, assuming a constant seepage rate onto Staten Island of 0.025 inches per foot rooting depth per month, and applying diversion and return rate limits.

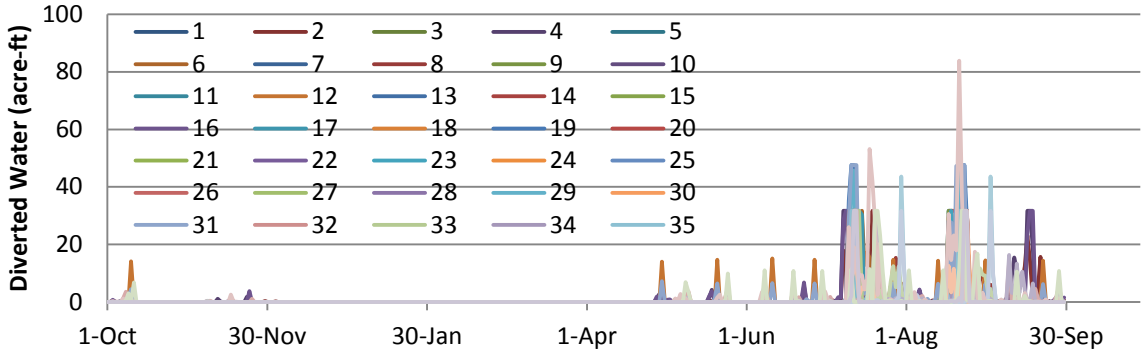

Figure 85. 2010, daily diverted water on Staten Island from ground-truthed diversion locations with limits applied to the diversion rate.

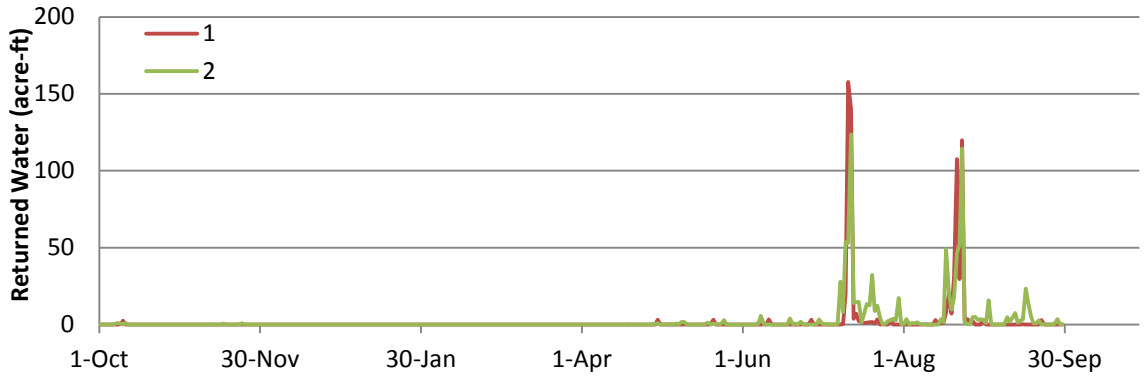

Figure 86. 2010, daily returned water on Staten Island from ground-truthed return locations with limits applied to the return rate.

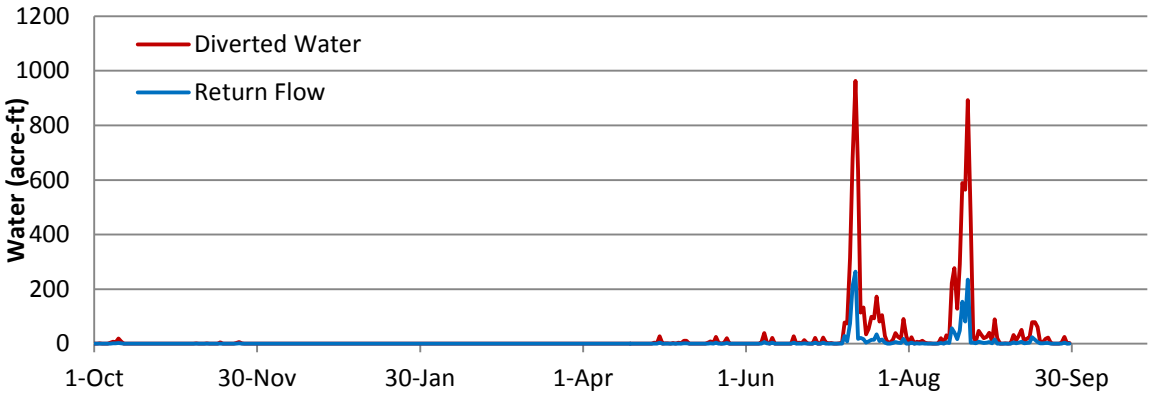

Figure 87. 2010, total daily diverted and returned water using a saturated hydraulic conductivity of 0.05 µm/s for all ponded elements, assuming a constant seepage rate onto Staten Island of 0.025 inches per foot rooting depth per month, and applying diversion and return rate limits

Appendix F: Horsepower Ratings of Pumps as Related to Unit-Use Coefficients in the Sacramento-San Joaquin Delta (Templin and Cherry 1997)

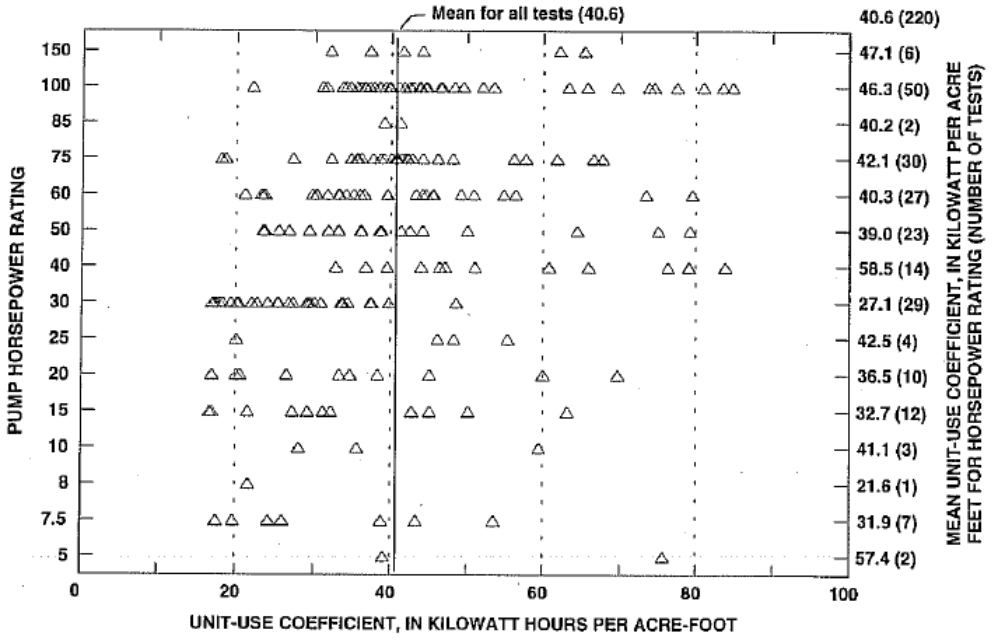

Figure 4. Horsepower ratings of pumps as related to unit-use coefficients derived from pump-efficiency tests for drains in the Sacramento-San Joaquin Delta, California.